



Synthesis, biological evaluation and molecular modelling of *N*-heterocyclic dipeptide aldehydes as selective calpain inhibitors

Matthew A. Jones^a, James D. Morton^{b,*}, James M. Coxon^a, Stephen B. McNabb^a, Hannah Y.-Y. Lee^b, Steven G. Aitken^a, Janna M. Mehrstens^a, Lucinda J. G. Robertson^b, Axel T. Neffe^{a,†}, Shigeru Miyamoto^a, Roy Bickerstaffe^b, Karl Gately^b, Jacqueline M. Wood^b, Andrew D. Abell^{a,*,‡}

^a Department of Chemistry, University of Canterbury, Private Bag 4800, Christchurch, New Zealand

^b Agriculture and Life Sciences Division, Post Office Box 84, Lincoln University, Canterbury, New Zealand

ARTICLE INFO

Article history:

Received 28 March 2008

Revised 21 May 2008

Accepted 22 May 2008

Available online 27 May 2008

Keywords:

Calpain

Isoform selectivity

Ovine calpain 1 and 2

In silico calpain homology model

Substituted heterocyclic dipeptides

CAT0059

ABSTRACT

A series of *N*-heterocyclic dipeptide aldehydes **4–13** have been synthesised and evaluated as inhibitors of ovine calpain 1 (o-CAPN1) and ovine calpain 2 (o-CAPN2). 5-Formyl-pyrrole **9** (IC₅₀ values of 290 and 25 nM against o-CAPN1 and o-CAPN2, respectively) was the most potent and selective o-CAPN2 inhibitor, displaying >11-fold selectivity. The amino acid sequences of o-CAPN1 and o-CAPN2 have been determined. Because of the lack of available structural information on the ovine calpains, in silico homology models of the active site cleft of o-CAPN1 and o-CAPN2 were developed based on human calpain 1 (h-CAPN1) X-ray crystal structure (PDB code 1ZCM). These models were used to rationalise the observed SAR for compounds **4–13** and the selectivity observed for **9**. The o-CAPN2 selective inhibitor **9** (CAT0059) was assayed in an in vitro ovine lens culture system and shown to successfully protect the lens from calcium-induced opacification.

© 2008 Elsevier Ltd. All rights reserved.

1. Introduction

Calpains are calcium activated neutral proteases belonging to the papain superfamily of cysteine proteases. The structure, mechanism of activation and pharmacological actions of calpain have been recently reviewed.¹ Over-activation of calpain is central to a number of medical conditions associated with cellular damage. These include traumatic brain injury, muscular dystrophy and cataract.² In the case of cortical cataract, increased lens calcium³ and subsequent over-activation of calpain 2 have been linked to the breakdown of lens proteins, resulting in clouding of the lens and ultimately blindness.^{4,5} Therefore, it has been proposed that devel-

opment of a potent and selective calpain 2 inhibitor would be a potential means of treating cortical cataract.

In this paper, we present SAR data on a series of *N*-heterocyclic peptidyl aldehydes **4–13** (see Schemes 1–3) that were designed to interact with the S3 binding pocket of calpains. Due to sequence differences between calpain 1 and 2 it was anticipated that the use of *N*-terminal heterocyclic moieties that interact differentially with either o-CAPN1 or o-CAPN2 would result in isoform selective calpain inhibitors.

A variety of *N*-terminal heterocyclic constituents of protease inhibitors have been shown to interact with key residues in the S3 hydrophobic pocket of cysteine proteases (Fig. 1). The quinoline derivative **1** was designed based on the expectation that the formation of additional hydrogen bonds might be possible via an interaction between the quinoline NH and calpain residues⁶; the P3 morpholine urea **2** exhibits a favourable electrostatic interaction with the sidechain ammonium group of Lys₆₄ in the S3 pocket of Cathepsin S⁷; and the extended P3 methylpiperazine-thiazolebenzamide **3** is capable of forming an ionic interaction to Asp₆₁ in the S3 pocket of Cathepsin K.⁸

In this paper, we extend this methodology by designing protease inhibitors with *N*-terminal heterocyclic moieties that are capable of preferentially binding o-CAPN2 over o-CAPN1, resulting in isoform selective calpain inhibitors.

Abbreviations: DIPEA, *N,N*-diisopropylethylamine; HATU, *O*-(7-azabenzotriazole-1-yl)-*N,N,N',N'*-tetramethyluronium hexafluorophosphate; pyr, pyridine; o-CAPN1, ovine calpain 1; o-CAPN2, ovine calpain 2; h-CAPN1, human calpain 1; h-CAPN2, human calpain 2; p-CAPN1, porcine calpain 1; p-CAPN2, porcine calpain 2; r-CAPN1, rat calpain 1; r-CAPN2, rat calpain 2.

* Corresponding authors. Tel.: +64 3 3253803x8169; fax: +64 3 3253851 (J.D. Morton); tel.: +61 8 8303 5652; fax: +61 8 8303 4358 (A.D. Abell).

E-mail addresses: mortonj@lincoln.ac.nz (J.D. Morton), andrew.abell@adelaide.edu.au (A.D. Abell).

[†] Present address: GKSS Research Centre, Institute of Polymer Research, Kantstrasse 55, 14513 Teltow, Germany.

[‡] Present address: School of Chemistry & Physics, The University of Adelaide, North Terrace, Adelaide, SA 5005, Australia.

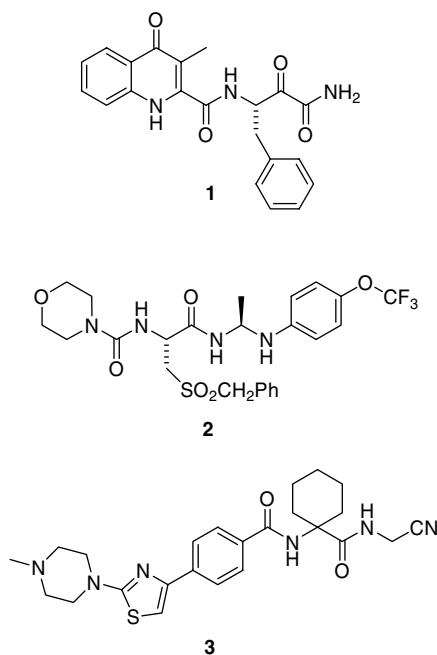


Figure 1. Protease inhibitors **1–3** designed to form hydrogen-bonding interactions in the S3 pockets of calpain, cathepsin S and cathepsin K, respectively.^{6–8}

Rodent models are most commonly used to assess the effect of anti-cataract agents.^{9–12} However, the rodent is a poor model for human cataract as its lenses are smaller, spherical, and have a different depth focus mechanism compared to human lenses.¹³ The ovine lens is a better model as it has a similar size, shape and accommodative index to the human lens.¹⁴ In addition, the ovine lens proteins are more similar to human lens proteins than those of the rat lens as shown by the close homology between sequences of ovine and human crystallins.¹⁵ For these reasons we have tested

the efficacy of the inhibitors using ovine calpains and an ovine lens culture assay.

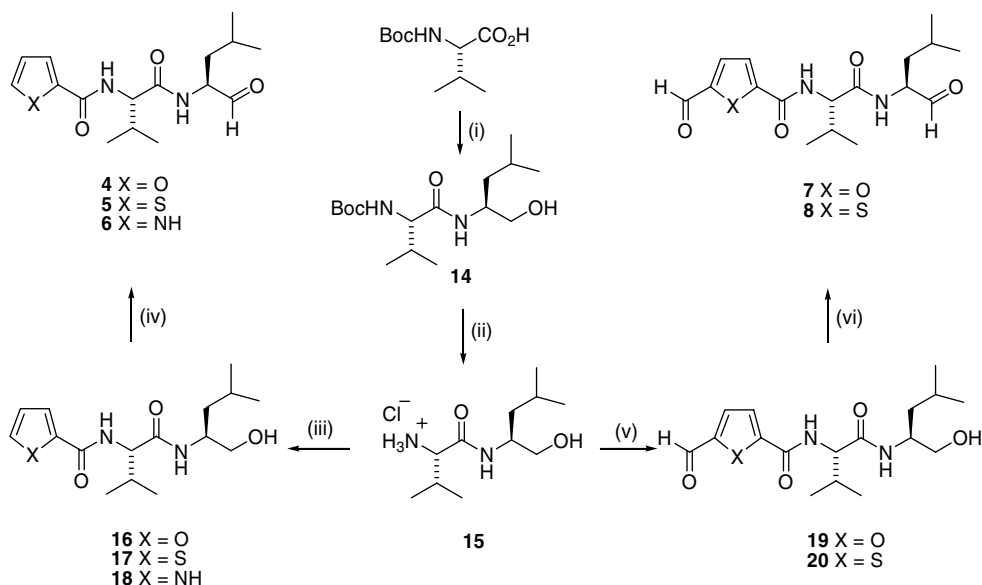
2. Results and discussion

2.1. Preparation of *N*-heterocyclic dipeptide aldehydes

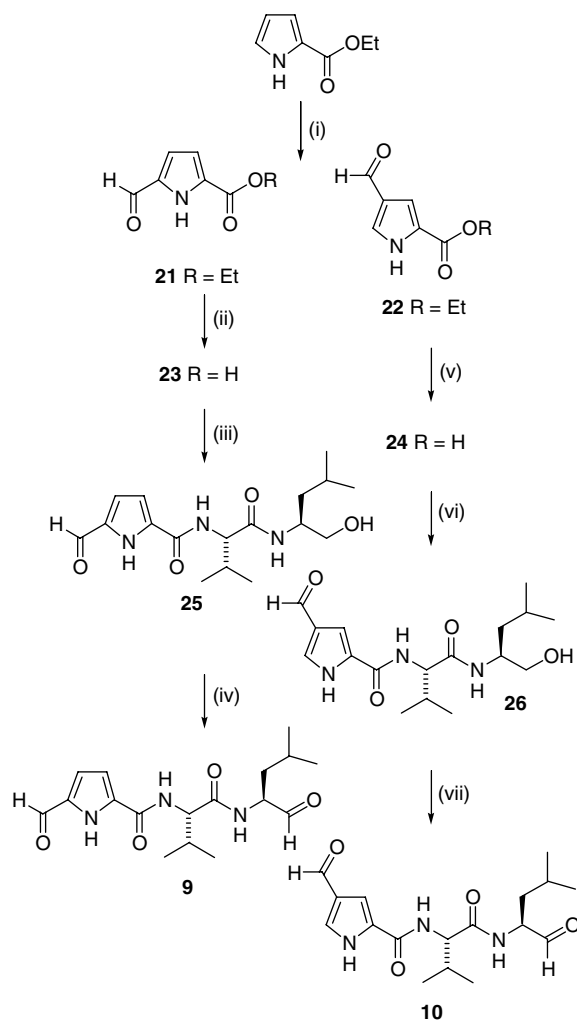
The target compounds **4–8** were prepared as detailed in Scheme 1. *N*-Boc-valine was reacted with *S*-leucinol to give the Boc protected dipeptide **14**. Treatment with HCl/dioxane gave the hydrochloride salt **15** in a quantitative yield.¹⁶ This key intermediate was separately reacted with five heterocyclic acids or acid chlorides to give the dipeptide alcohols **16–20**.¹⁷ Subsequent oxidation of the alcohols **16–20** with SO₃-pyridine (SO₃-pyr) and DMSO (the Parikh–Doering¹⁸ oxidation reaction) gave the aldehydes **4–8** in good yields (Scheme 1).

Aldehydes **9** and **10** were prepared as described in Scheme 2. Formylation of 2-pyrrole carboxylic acid ethyl ester gave a mixture of 5- and 4-formyl-pyrrole ethyl ester isomers **21** and **22** (2.4:1) that were separable by chromatography.¹⁹ Separate ester hydrolysis of ester isomers **21** and **22** resulted in the formation of 5-formyl-2-pyrrole carboxylic acid **23** and 4-formyl-2-pyrrole carboxylic acid **24**, respectively. The acids **23** and **24** were reacted with **15** to give the alcohols **25** and **26**. Oxidation gave the corresponding aldehydes **9** and **10** (Scheme 2).

Aldehydes **11–13** were prepared as described in Scheme 3. The substituted 2-pyrrole carboxylic acid precursors **27–29** were synthesised using standard literature procedures.^{20,21} 5-Formyl-*N*-methyl-pyrrole-2-carboxylic acid **27** was synthesised via alkylation of 2-pyrrole carboxylic acid using methyl iodide and NaOH followed by base-mediated ester hydrolysis.²⁰ 5-Methyl-pyrrole-2-carboxylate **28** was synthesised from the reaction of diethyl acetamidomalonate and 1,4-dichloro-2-butyne using NaOEt as a base in refluxing EtOH according to the method developed by Curran and Keaney²¹ followed by ester hydrolysis. 5-Methoxycarbonyl-2-pyrrole carboxylic acid **29** was synthesised via KMnO₄ oxidation of the corresponding 5-formyl ester in methanol.²⁰ The pyrrole acids **27–29** were



Scheme 1. Synthesis of inhibitors **4–8**. Reagents: (i) *S*-leucinol, HATU, DIPEA, DMF (68%); (ii) 4 M HCl/dioxane (99%); (iii) DIPEA, DMF, 2-furan-carbonyl chloride or 2-thiophene-carbonyl chloride or (2-pyrrole-carboxylic acid and HATU) (48%, 56% and 84%, respectively); (iv) SO₃-Pyr, DMSO, DCM, DIPEA (58%, 51% and 71%, respectively); (v) DIPEA, DMF, HATU 5-formyl-2-furan-carboxylic acid or 5-formyl-2-thiophene-carboxylic acid (30% and 88%, respectively); (vi) SO₃-Pyr, DMSO, DCM, DIPEA (80% and 89%, respectively).



Scheme 2. Synthesis of inhibitors **9** and **10**. Reagents: (i) POCl₃, DMF (**21**, 59%; **22** 25%); (ii) NaOH, MeOH, H₂O (93%); (iii) HATU, DIPEA, DMF, **15** (39%); (iv) SO₃-Pyr, DMSO, DCM, DIPEA (71%); (v) NaOH, THF, H₂O (85%); (vi) HATU, DIPEA, DMF, **15** (36%); (vii) SO₃-Pyr, DMSO, DCM, DIPEA (90%).

reacted with **15** to give alcohols **30–32** that were oxidised to give the corresponding aldehydes **11–13** (Scheme 3).

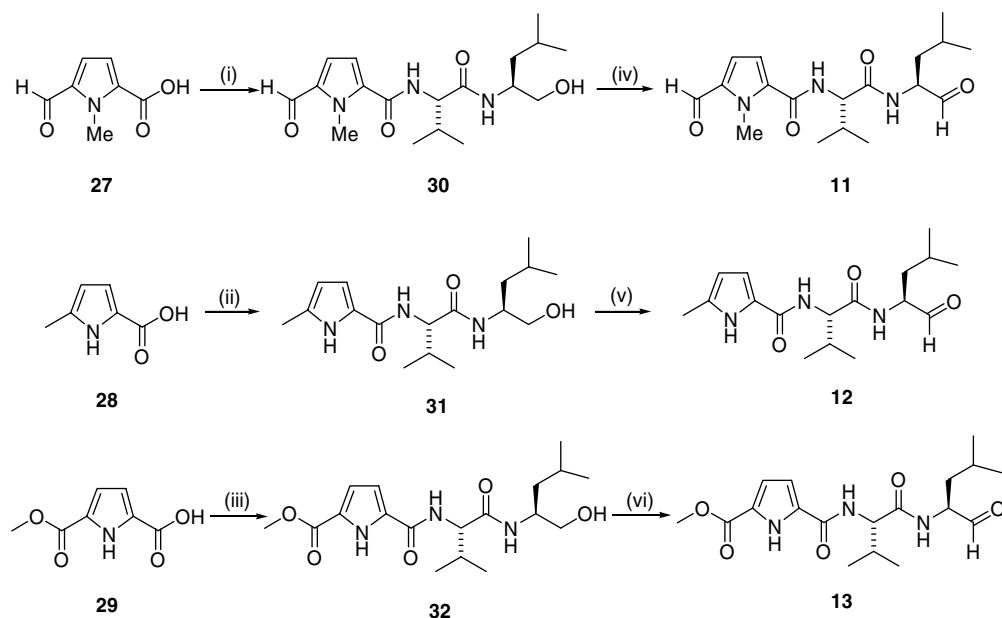
2.2. Ovine calpain sequence

The amino acid sequences of the catalytic subunits of o-CAPN1 and o-CAPN2 were deduced from their cDNA sequences (GenBank Accession Nos. EU623071 and EU161096, respectively). o-CAPN2 has two alleles with a G replaced by a T at 741 and a C replaced by a T at 1539. However, neither of these alter the amino acid sequence. The human calpain sequences, h-CAPN1²² and h-CAPN2,²³ are more homologous to the ovine calpains, o-CAPN1 and o-CAPN2, than to the rat calpains, r-CAPN1²⁴ and r-CAPN2.²⁵ The o-CAPN1 amino acid sequence is 95% homologous with the h-CAPN1, considerably closer than the 89% homology of r-CAPN1 to h-CAPN1. The large subunits of o-CAPN2 and h-CAPN2 are 95% homologous. This compares with 94% for rat with human. Of the 35 amino acids which differ between o-CAPN2 and h-CAPN2, 18 are conservative substitutions (similar amino acids) and the changes are clustered in non-essential regions of the protein. The homology between o-CAPN2 and o-CAPN1 is 62%, which is similar to that found in other species. o-CAPN2 is also 62% homologous to h-CAPN1.

Alignment of selected residues in the catalytic domain of ovine, human and rat calpain highlights the greater homology between ovine calpains and h-CAPN1 compared to r-CAPN1 (Fig. 2). Within these sections there are 11 amino acids different between h-CAPN1 and r-CAPN1 and only two between h-CAPN1 and o-CAPN1. There are nine differences between h-CAPN1 and o-CAPN2. However, only two of these differences occur in proximity to the active site, namely Ser₂₀₉ and Met₂₆₀ in h-CAPN1, which correspond to Ala₁₉₉ and Ser₂₅₀ in o-CAPN2, respectively.

2.3. Biological activity

The compounds **4–13** were assayed against o-CAPN1 and o-CAPN2, purified from ovine lung tissue, using a fluorescence-based assay to determine in vitro potency and selectivity,²⁶ and the results summarised in Table 1. All compounds inhibited both o-CAPN1 and o-CAPN2 with IC₅₀ values below 1 μM. 5-Formylpyrrole **9** (IC₅₀ values of 290 and 25 nM against o-CAPN1 and



Scheme 3. Synthesis of inhibitors **11–13**. Reagents: (i) **15**, HATU, DIPEA, DMF (56%); (ii) **15**, HATU, DIPEA, DMF, (29%); (iii) **15**, HATU, DIPEA, DMF (64%); (iv) SO₃-Pyr, DMSO, DCM, DIPEA (75%); (v) SO₃-Pyr, DMSO, DCM, DIPEA (63%); (vi) SO₃-Pyr, DMSO, DCM, DIPEA (69%).

r-CAPN1	1	M EE F ITPVY	CTGVSAQVQK	QR D KLGLGR	HENAIKYLQ	DYENLR A RCL	QNGVLFQ D DA	FPVP S SLGF	70
h-CAPN1	1	MSE E ITPVY	CTGVSAQVQK	QRARELGLGR	HENAIKYLQ	DYEQLRV R CL	QSGTLFRDEA	FPVPQ S SLGY	70
o-CAPN1	1	M EE F ITPVY	CTGVSAQVQK	QRA K ELGLGR	HENAIKYLQ	DYEQLRVH C L	QRGALFRDEA	FPVPQ S SLGF	70
o-CAPN2	1	M AGIA A KLAK	D REAA E GLGS	HERA K YLNQ	DYAA L RDECL	E AGAL F QDPS	FP A LP S SLGF	60
r-CAPN1	71	K ELGPNSSKT	YGIKWKRPT E	LLSNPQFIVD	GATRTD I CQ G	AL G DCWLLAA	IASLT L NETI	LHRVVP V QGS	140
h-CAPN1	71	KDLGPNSSKT	YGIKWKRPT E	LLSNPQFIVD	GATRTD I CQ G	AL G DCWLLAA	IASLT L NDTL	LHRVVP H QGS	140
o-CAPN1	71	K ELGPNSSKT	YGIKWKRPT E	LFSNPQFIVD	GATRTD I CQ G	AL G DCWLLAA	IASLT L NDTL	LHRVVP H QGS	140
o-CAPN2	61	K ELGPYSSKT	R GI E WKRPTE	I CDDPQFIT G	GATRTD I CQ G	AL G DCWLLAA	IASLT L NEET	LARVVP L DQS	130
r-CAPN1	141	FQEGYAGIFH	FQLWQFGEW V	DVVVDDLL P T	KDGKLVFVHS	AQ G NEFW S AL	LEKAYAKVNG	SYEAL S GG C T	210
h-CAPN1	141	FQNGYAGIFH	FQLWQFGEW V	DVVVDDLL P I	KDGKLVFVHS	AEGNEFW S AL	LEKAYAKVNG	SYEAL S GG S T	210
o-CAPN1	141	FQDGYAGIFH	FQLWQFGEW V	DVVVDDLL P T	KDGKLVFVHS	AQ G NEFW S AL	LEKAYAKVNG	SYEAL S GG S T	210
o-CAPN2	131	FQENYAGIFH	FQF W QYGEW V	E VVVDDLL P T	KD G EL L FVHS	AEG S EFW S AL	LEKAYAK I NG	C YEAL S GG A T	200
r-CAPN1	211	SEAFEDFTGG	VTEWY L QKA	PSDLYQIILK	ALERGSLLGC	S INIS D IR D L	EAITFK N LV R	G HAYS V T D AK	280
h-CAPN1	211	SEGFEDFTGG	VTEWYELRKA	PSDLYQIILK	ALERGSLLGC	S IDISSV L DM	EAITFK K LV K	G HAYS V T G AK	280
o-CAPN1	211	SEGFEDFTGG	VTEWYELRKA	PSDLYIILK	ALERGSLLGC	S IDISS I DM	EA V TF K LV K	G HAYS V T G AK	280
o-CAPN2	201	T EGFEDFTGG	I AEWYELRKA	P PN L FR I IQ K	AL O KGSLLGC	S ID I T S AA S	EAIT F C K LV K	G HAYS V T G A E	270
r-CAPN1	281	QV T Y Q Q R V N	LIRMRNPWGE	VEW K GEWSD N	S YEW N KVDPY	EREQLRVKME	DGEFWMSFRD	F IREFT K LE I	350
h-CAPN1	281	QVNYRQ Q V S	LIRMRNPWGE	VEWTGAWS D S	S SEWN N VDPY	ERDQLRVKME	DGEFWMSFRD	F MREFT R LE I	350
o-CAPN1	281	QVNY Q Q C M V N	LIRMRNPWGE	VEWTGAWS D C	S SEWN G VDPY	V REQL R IKME	DGEFWMSFRD	F MREFT R LE I	350
o-CAPN2	271	E VESRG S L O K	LIR I RNPWGE	VEWT G W N D N	C PNW N TVD P E	V RES L TRR H E	DGEFWMS F S	F LR H YS R LE I	340
r-CAPN1	351	CNLTDPALKS	RTL R NWNT T F	YEGTWRRGST	AGGCRNYPAT	FWVNPQFKIR	LEE V DDADDY	D S . .RESGCS	418
h-CAPN1	351	CNLTDPALKS	RTIRKWNT T L	YEGTWRRGST	AGGCRNYPAT	FWVNPQFKIR	LDETDDDDY	G D . .RESGCS	418
o-CAPN1	351	CNLTDPALKS	QRFR N WNT T L	YEGTWRRGST	AGGCRNYPAT	FWVNPQFKIR	LEETDDPD P D	D YGGRESGCS	420
o-CAPN2	341	CNLTDP L LT S	D TYKKW K L T K	M DG N WRRGST	AGGCRNYP N T	FWNPQV L IK	LEE D EDQ D E	G .. . ESG C T	406
r-CAPN1	419	F LLALMQKHR	RRERRFGRDM	ETIGFAVY Q V	P REL A G P . V	HLKRDFFLAN	ASRA Q SE H FI	NLREVS N R I R	487
h-CAPN1	419	FVLALMQKHR	RRERRFGRDM	ETIGFAVY E V	P PELVQ G PAV	HLKRDFFLAN	ASRARSEQ F I	NLREVSTR F R	488
o-CAPN1	421	F LLALMQKHR	RRERRFGRDM	ETIGFAVY E V	P PELVQ G PAV	HLKRDFFLAN	ASRARSEQ F I	NLREVSTR F R	490
o-CAPN2	407	F LVGL I QKHR	RR R K M G E DM	H TIG F GIY E V	P EE F T G Q T N I	H LS K K F FL T T	R AR E RS D T F I	NLREVL N R F K	476
r-CAPN1	488	LPPGEY I VVP	STFEPNKEGD	F LLRFFSE K K	AGT Q ELDDQ I	QANLPDE K VL	SEEEID N FK	T LF S KLAG D D	557
h-CAPN1	489	LPPGEYVVVP	STFEPNKEGD	FVLRFFSE K S	AGTVELDDQ I	QANLPDEQVL	SEEEIDEN F K	ALFRQLAG E D	558
o-CAPN1	491	LPPGEYVVVP	STFEPNKEGD	FVLRFFSE K S	AGT Q ELDDQ V	QANLPDEQVL	SEEEIDEN F K	S LF R QLAG E D	560
o-CAPN2	477	LPPGEY I VVP	STFEPNK D G D	F CIR V FSE K K	ADYQV V DD E I	E AN L EE I D I	SEDDID D G F R	R L F AQLAG E D	545
r-CAPN1	558	MEISVKEL Q T	ILNRIISKHK	DLRT N GFS L E	SCRSMVN L MD	RDGNGKLGLV	EFNILWN R IR	NYL T IFR K FD	627
h-CAPN1	559	MEISVKELRT	ILNRIISKHK	DLRTKGFS L E	SCRSMVN L MD	RDGNGKLGLV	EFNILWN R IR	NYLSIFR K FD	628
o-CAPN1	561	MEISVKELRT	ILNRIISKHK	DLRT T GFS V E	SCRSMVN L MD	RDGNGKLGLV	EFNILWN R IR	NYLSIFR K FD	630
o-CAPN2	546	A EIS A EL Q T	ILRRV L AK R O	DIKSDGFS I E	T CKIMV D ML D	S DGS G KLGL K	EFYILW T K I O	K YQ K IY R E I D	615
r-CAPN1	628	LDKSGSMSAY	EMRMAIE A AG	FKLNKK L HEL	IITRYSEPD L	AVDFDNFVCC	LVRLET M FRF	F K I LDTDL D LG	697
h-CAPN1	629	LDKSGSMSAY	EMRMAIE S AG	FKLNKK L YEL	IITRYSEPD L	AVDFDNFVCC	LVRLET M FRF	F K T LDTDL D LG	698
o-CAPN1	631	LDKSGSMSAY	EMRMAIE F AG	FKLNKK L YEL	IITRYSEPD L	AVDFDNFVCC	LVRLET M FRF	F K T LDTDL D LG	700
o-CAPN2	616	V DRSG T M S Y	EMRK A IE A AG	FKMP C Q L H Q V	I VAR F AD D DL	I ID F DNF V RC	L IRLET L FR I	F K Q LD P ENT G	685
r-CAPN1	699	VVTFDLFKWL	QLTMFA	713	Genbank accession number: NM019152				
h-CAPN1	700	VVTFDLFKWL	QLTMFA	714	NM005186				
o-CAPN1	701	VVTFDLFKWL	QLTMFA	716	EU623071				
o-CAPN2	687	M IQ L DL I SW L	C FS V L	700	EU161096				

Figure 2. Sequence alignment of r, h and o-CAPN1, and o-CAPN2. Amino acid residues forming part of the active site cleft and binding pockets are in bold type. Amino acid substitutions compared to h-CAPN1 are shaded.

Table 1
In vitro inhibition data

Compound	IC ₅₀ ^a (nM)		Selectivity o-CAPN2 over o-CAPN1
	o-CAPN1	o-CAPN2	
4	790	135	5.85
5	680	100	6.80
6	650	315	2.06
7	960	100	9.60
8	440	85	5.18
9	290	25	11.6
10	530	100	5.30
11	150	150	1.00
12	340	110	3.09
13	290	140	2.07

^a Values are means of three experiments. Variation between experiments is $\leq 10\%$.

o-CAPN2, respectively) was the most potent and selective o-CAPN2 inhibitor, displaying >11-fold selectivity. In contrast, other well-documented dipeptidyl aldehyde calpain inhibitors such as SJA6017²⁷ (IC₅₀ values of 7.5 and 78 nM against porcine calpain 1 (p-CAPN1) and porcine calpain 2 (p-CAPN2), respectively) and MDL28170²⁸ (IC₅₀ values of 56 and 350 nM against h-CAPN1 and h-CAPN2, respectively) display selectivity for calpain 1 over calpain 2. Formyl-furan **7** (IC₅₀ values of 960 and 100 nM against o-CAPN1 and o-CAPN2, respectively) was also a highly potent and selective o-CAPN2 inhibitor, displaying >9-fold selectivity for o-CAPN2 compared to o-CAPN1. The inhibitors **4–6**, **8**, **10**, **12** and **13** displayed moderate selectivity (between 2- and 7-fold) for o-CAPN2, while *N*-methyl-pyrrole **11** was non-selective.

Compounds **4–10**, **12** and **13** are all more potent against o-CAPN2 than o-CAPN1 (Table 1). The assay results for o-CAPN1

(Table 1) show that the pyrrole containing derivatives, **6** and **9–13**, are generally more potent than the furan or thiophene analogues **4**, **5**, **7** and **8**. A 5-carbonyl substituent on pyrrole (**9**, **11**, **13**) appears to be important for optimum activity against o-CAPN1, as pyrrole analogues lacking this group (**6**, **10** and **12**) show reduced potency. It is also noteworthy that the 5-formyl and 5-methoxycarbonyl pyrrole derivatives **9** and **13** are equally potent against o-CAPN1. In addition, the *N*-methyl-pyrrole derivative **11** is more potent against o-CAPN1 than its unsubstituted analogue **9**.

The assay results show the 5 formyl thiophene **8** and 5-formyl-pyrrole **9** to be the most potent analogues against o-CAPN2. The importance of a 5-carbonyl substituent parallels the o-CAPN1 assay results. The *N*-methyl-pyrrole **11** is less potent against o-CAPN2 than the unsubstituted analogue **9**. This order of potency is the reverse of that observed for o-CAPN1.

2.4. Construction of in silico ovine calpain homology models

Molecular modelling was used to rationalise the observed SAR of compounds **4–13**. Novel in silico ovine calpain homology models were constructed using the o-CAPN1 and o-CAPN2 sequences and h-CAPN1 X-ray crystal structure data available from the Protein Data Bank (PDB code 1ZCM).²⁹

The most appropriate calpain X-ray crystal structure information is required to build accurate in silico ovine calpain models. Ten X-ray crystal structures of the active catalytic domains of calpains 1 and 2 have been published.³⁰ Eight of these crystal structures have been obtained by Davies using a rat calpain 1 (r-CAPN1) construct. Unfortunately, no useful structural information is available for the rat calpain 2 (r-CAPN2) construct due to an instability in helix $\alpha 7$, which results in intrinsic inactivation.³¹ Only two h-CAPN1 construct crys-

tal structures have been published^{29,32}; however, one is in an inactive form.³² The sequence alignment of selected residues of h-CAPN1,²² r-CAPN1,²⁴ o-CAPN1 and o-CAPN2 clearly shows that a high degree of homology exists within the residues that form the active site cleft of ovine calpains and h-CAPN1 (Fig. 2). Therefore, h-CAPN1 X-ray crystal structure (1ZCM) was used as the structural basis for the o-CAPN1 homology model.

A similar strategy was employed to build the o-CAPN2 homology model. Despite a number of differences in the amino acid sequence of h-CAPN1 and o-CAPN2 (Fig. 2), it was decided to build the in silico o-CAPN2 homology model based on the h-CAPN1 X-ray crystal structure (1ZCM)²⁹ as this is the most appropriate X-ray crystal structure available. Therefore, the model based on this X-ray structure is likely to be the best available to rationalise the observed SAR of compounds **4–13**.

2.5. Molecular modelling and SAR discussion

The h-CAPN1 X-ray crystal structure, 1ZCM, was mutated in silico around the active site cleft to mimic the amino acid sequence of either o-CAPN1 or o-CAPN2 (see Section 4.5). These two ovine calpain homology models were then used to dock compounds **4–13**.^{33,34}

Aldehyde inhibitors of cysteine proteases are considered to act by reversible formation of a thio-hemiacetal. Docking studies with Glide³⁴ do not allow for covalent bond formation between the cysteine thiol and the aldehyde. The potential inhibitor and enzyme necessarily remain as separate molecular entities. Such studies allow the potential of a compound to position itself to act as an inhibitor to be evaluated. They show whether or not the aldehyde carbonyl carbon is positioned appropriately for attack by the

Table 2

Docking results and parameter for compounds **4–13**

Compound	Grid	No. starting conf.	No. poses generated	No. poses with WHD < 4.5 ^a	Most representative pose			
					H bonds ^{b,c}	WHD ^a	E _{model}	E _{internal}
4	OvineI	4	39	36	A, B, Ser ₂₅₁	3.38	−56.04	4.48
	OvineII		34	34	A, C	3.31	−47.95	5.84
5	OvineI	3	27	20	B, C, Ser ₂₅₁	3.67	−52.03	1.78
	OvineII		22	17	B, C, Gly ₂₆₁	3.47	−53.65	7.87
6	OvineI	4	40	17	B, C	3.72	−50.55	4.26
	OvineII		40	26	B, C, Ser ₂₆₁	3.46	−50.44	4.91
7	OvineI	4	40	19	B, C	4.02	−54.27	6.42
	OvineII		32	7	A, B, C, Ile ₂₄₄	3.81	−50.65	6.84
8	OvineI	5	35	28	A, B, C	3.97	−54.54	5.58
	OvineII		49	44	A, B, C	3.69	−49.40	5.23
9	OvineI	4	40	27	A, B, C, Ile ₂₅₄	4.15	−53.66	1.15
	OvineII		32	6	Gln ₉₉ , Gly ₂₆₁ , 2 × Gly ₁₉₈	3.54	−50.49	3.69
10	OvineI	4	37	16	B, C	4.17	−50.86	3.72
	OvineII		32	23	B, C	3.46	−55.13	3.83
11	OvineI	3	30	23	A, B, C, Ile ₂₅₄	3.72	−54.05	5.84
	OvineII		17	13	A, B, C, Ile ₂₄₄	3.74	−52.95	6.96
12	OvineI	3	17	8	B, C, Thr ₂₁₀	3.54	−56.14	4.86
	OvineII		27	8	C, Gly ₂₇₁	3.48	−53.94	3.66
13	OvineI	4	34	9	A, B, C, Ile ₂₅₄	4.40	−54.76	3.81
	OvineII		36	15	B, C, Ile ₂₄₄	3.47	−53.39	2.74

^a War head distance (WHD) is the distance between the carbonyl carbon of the aldehyde and the active site cysteine sulfur in Å.

^b Hydrogen bonds from the carbonyl group of Gly₂₀₈, the NH group of Gly₂₀₈ and the carbonyl group of Gly₂₇₁ of the o-CAPN1 homology model are labelled A, B and C, respectively.

^c The analogous hydrogen bonds from the carbonyl group of Gly₁₉₈, the NH group of Gly₁₉₈, and the carbonyl group of Gly₂₆₁ of the o-CAPN2 homology model are also labelled A, B and C, respectively.

nucleophilic sulfur of the cysteine as required for the compound to act as a reversible covalent inhibitor.

Modelling studies show the inhibitors **4–8** and **10–13** are docked in the o-CAPN1 and o-CAPN2 models in a similar conformation, orientation and hydrogen-bonding arrangement (Table 2, see Section 4) to that observed in the crystal structures of leupeptin and SNJ1715 each co-crystallised in r-CAPN1.^{35,36} The inhibitors **4–13** can be divided into three groups based on the observed selectivity for o-CAPN2 over o-CAPN1: **4–6**, **8**, **10**, **12** and **13** display moderate isoform selectivity (2- to 7-fold); **7** and **9** are the most selective (9.60- and 11.6-fold, respectively); while **11** is non-selective.

The inhibitor conformations, orientations and hydrogen-bonding arrangements for each of **4–6**, **8**, **10**, **12** and **13** are similar for the two calpain models. This similarity could explain why the potency of each inhibitor is comparable in o-CAPN1 and o-CAPN2 and why the inhibitors only display moderate isoform selectivity (Table 1). For example, the representative poses³⁷ of **8** in the o-CAPN1 and o-CAPN2 models show that the inhibitor is in a β -strand conformation. The most representative poses of **8**, with o-CAPN1 and with o-CAPN2, are shown in Figure 3a and b, respectively. The carbonyl carbon of the C-terminal aldehyde, in the representative poses for **8** with o-CAPN1 and o-CAPN2, is positioned to allow for attack by the nucleophilic sulfur of the active site cysteine. Here the distance between the carbonyl carbon and the active site cysteine sulfur is 3.97 Å and 3.44 Å, respectively.

Representative poses of the most selective inhibitors **7** and **9** (Table 1) appear to have different inhibitor conformations in each

of the o-CAPN1 and o-CAPN2 models. For example, the representative poses of **9** in the o-CAPN1 model show the inhibitor in a β -strand conformation. The most representative pose is shown in Figure 3c. The representative poses³⁸ of **9** in o-CAPN2 show the inhibitor is in a unique shunted arrangement and conformation.³⁹ The most representative pose is shown in Figure 3d. The two poses (Fig. 3c and d) have similar Glide *E*_{model}⁴⁰ scores (–53.66 and –50.49, respectively) and Glide *E*_{internal}⁴¹ scores (1.15 and 3.69 kJ, respectively). This suggests that the shunted arrangement of **9** (Fig. 3d) is of similar energy to the more common β -strand binding mode (Fig. 3c). The most representative shunted arrangement of **9** (Fig. 3d) has the carbonyl carbon of the C-terminal aldehyde in proximity to the active site cysteine (3.54 Å) with an additional hydrogen bond between the aldehyde oxygen and Gln₉₉. A hydrogen bond is also formed between the pyrrole –NH and Gly₁₉₈ (Table 2, see Section 4).

For the non-selective inhibitor **11**, the most representative poses in the o-CAPN1 and o-CAPN2 models are almost identical. This is consistent with its equal potency against o-CAPN1 and o-CAPN2 (Table 1).

The similar potency of 5-formyl-pyrrole **9** and its *N*-methyl derivative **11** against o-CAPN1 (Table 1) is consistent with a common mode of binding. However, the uniquely shunted arrangement and conformation of **9** bound to o-CAPN2 (as discussed above) contrasts the more common β -strand inhibitor conformation observed for **11**. This may explain the enhanced potency of **9** against o-CAPN2.

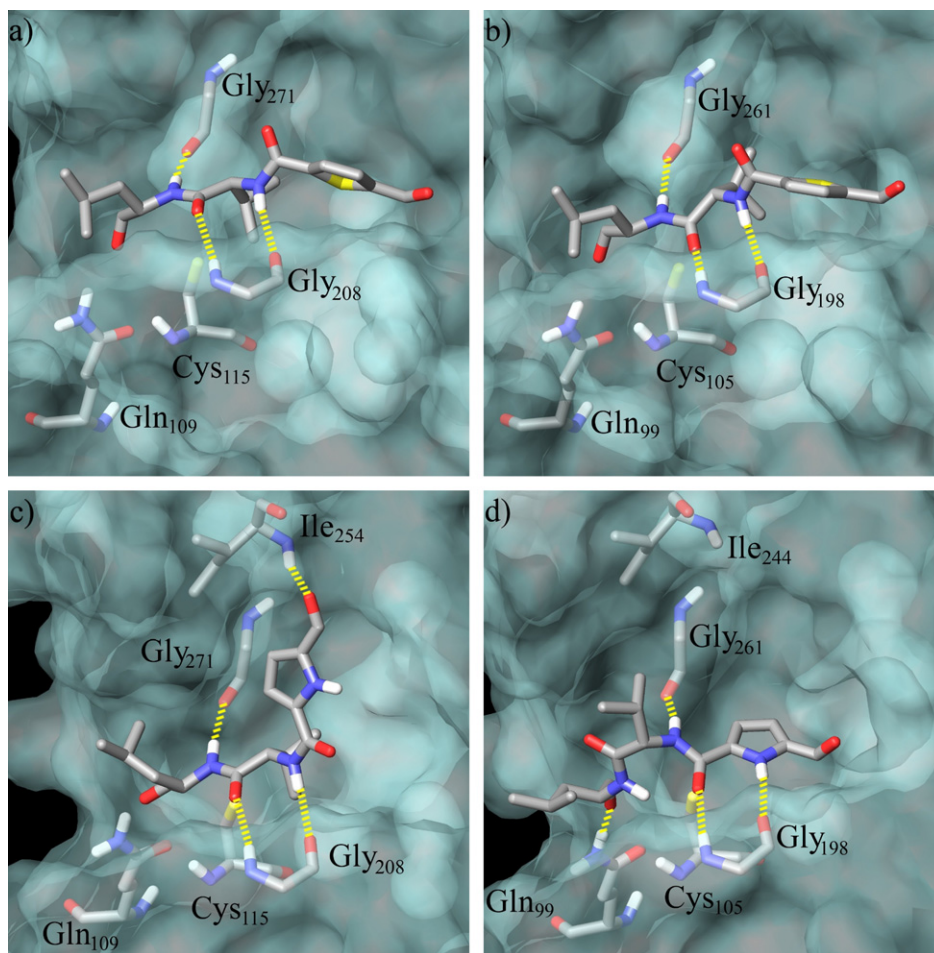


Figure 3. Most representative poses of **8** docked to (a) o-CAPN1 homology model in a β -strand conformation and (b) o-CAPN2 homology model in a β -strand conformation and **9** docked to (c) o-CAPN1 homology model in a β -strand conformation and (d) o-CAPN2 homology model in a unique shunted arrangement. The parameters for the representative poses of **4–13** docked into the o-CAPN1 and o-CAPN2 homology models are shown in Table 2 in Section 4.

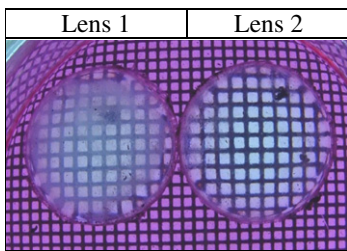
Lens 1	Lens 2
	
Mean opacification grading score (\pm sd)	
45.1 \pm 2.9	27.9 \pm 5.5

Figure 4. Calcium-induced cataract in ovine lenses. The scores represent the average result using three lens pairs. Opacification scores of 100 = full opacity, whereas a score of 1 = clear and transparent. The loss of transparency was significantly reduced by o-CAPN2 selective inhibitor **9**.

2.6. In vitro lens culture assay

Overactivation of calpain 2 has been linked to the development of cortical cataract hence the o-CAPN2 selective inhibitor **9** was assayed in an in vitro lens culture system. The ability of **9** to retard calpain-induced cell damage in ovine lenses was studied. A detailed method for this assay has been previously reported.¹⁶ Inhibitor **9** (10 μ M) was added to one lens from each pair of sheep lenses in culture media. After 2 h incubation, calcium was added to all lenses to activate the constituent calpains and induce cataract formation. After 44 h all lenses were photographed and the opacity graded; see Figure 4 for a representative pair of lenses. Lenses treated with calcium only (e.g., lens 1 in Fig. 4) clearly showed the opacity associated with cataract formation; however, lenses treated with calcium in the presence of **9** (e.g., lens 2) remained essentially transparent, as revealed by the reference grid placed behind each lens. The loss of transparency was significantly reduced by **9** ($p < 0.005$ in a paired t -test).

3. Conclusion

A range of N-terminal heterocyclic dipeptide aldehydes **4–13**, designed to interact with the S3 binding pocket of calpain, have been prepared and assayed in vitro against o-CAPN1 and o-CAPN2. Compounds **4–13** are potent calpain inhibitors with IC_{50} values below 1 μ M and show differing degrees of isoform selectivity. The 5-formyl-pyrrole **9** was highly active against o-CAPN2 (IC_{50} 25 nM) and exhibited >11-fold selectivity for o-CAPN2 over o-CAPN1. In contrast, other documented dipeptidyl aldehyde calpain inhibitors such as SJA6017 and MDL28170 display selectivity for calpain 1 over calpain 2.

The amino acid sequences of catalytic subunits of o-CAPN1 and o-CAPN2 were deduced from their cDNA sequences and have 95% homology to the analogous human isoforms. In silico homology models were generated from the o-CAPN1 and o-CAPN2 sequences and h-CAPN1 X-ray crystal structure data. The models have been used to rationalise the observed SAR of compounds **4–13**. The observation that the representative poses of **9** in o-CAPN2 show the inhibitor in a unique shunted arrangement and different from all other inhibitor poses in both calpain models could explain the high isoform selectivity (>11-fold) of this inhibitor for o-CAPN2 over o-CAPN1.

The o-CAPN2 selective inhibitor **9** was assessed in an in vitro lens culture assay and shown to successfully protect the lens from calcium-induced opacification. Development of **9** (CAT0059) is ongoing⁴² and its suitability for use as an in vivo anti-cataract agent will be reported in a future publication.

4. Experimental

4.1. Chemistry

Proton NMR spectra were acquired on a Varian Inova 500 spectrometer recorded at 500 MHz unless otherwise stated. Carbon NMR spectra were obtained on a Varian Unity XL 300 MHz Fourier Transform spectrometer recorded at 75 MHz with a delay (D_1) of 1 s. Unless otherwise stated, all spectra were obtained at 23 °C. Chemical shifts are reported in parts per million (ppm, δ) and are referenced relative to residual solvent, for example, $CDCl_3$ ($CHCl_3$ at δ_H 7.26 ppm). Electrospray ionisation (ESI) mass spectra were detected on a micromass LCT TOF mass spectrometer with a probe voltage of 3200 V and a source temperature of 80 °C. Infrared spectra were obtained using a Shimadzu 9201PC series FTIR interfaced with an Intel 486 PC operating Shimadzu HyperIR software. Diffuse reflectance spectra were obtained in a solid KBr matrix. Melting points were obtained on an electrothermal melting point apparatus and are uncalibrated. Microanalysis was performed at the University of Otago Microanalytical Laboratory. All reported values are within $\pm 0.4\%$ of the calculated value. Thin layer chromatography (TLC) was performed on aluminium-backed Merck Kieselgel KG60F silica plates and flash column chromatography was carried out under a positive pressure of dry nitrogen using Merck silica gel 60 (230–400 mesh). All chemicals were purchased from Aldrich in the highest possible purity.

4.1.1. General procedure A: amide bond formation from an acid chloride

To a stirred solution of the acid chloride (1.0 equiv) in dry *N,N*-dimethylformamide were added the amine (1.0 equiv) and DIPEA (2.0 equiv), and the resulting solution was stirred at rt overnight. The reaction mixture was diluted with ethyl acetate and washed successively with aqueous 1 M HCl, saturated aqueous sodium bicarbonate and brine. The organic phase was separated, then dried over $MgSO_4$ and concentrated in vacuo.

4.1.1.1. Furan-2-carboxylic acid [(S)-1-((S)-1-hydroxymethyl-3-methyl-butylcarbamoyl)-2-methyl-propyl]-amide (16). To a stirred solution of **14** was added 4 M HCl in dioxane (10.0 equiv), and the resulting solution was stirred at rt overnight. Concentration in vacuo gave the hydrochloride salt **15**, which was used subsequently without further purification. Reaction of **15** with 2-furan-carbonyl chloride according to general procedure A gave **16** as a colourless oil (0.15 g, 48%). HRMS (ES^+) calcd for $C_{16}H_{27}N_2O_4$ ($M+H^+$) 311.1971 found 311.1973; 1H NMR (500 MHz, CD_3OD) 0.85 (3H, d, $J=6.4$ Hz, CH_3), 0.87 (3H, d, $J=6.4$ Hz, CH_3), 0.98 (3H, d, $J=6.8$ Hz, CH_3), 1.00 (3H, d, $J=6.8$ Hz, CH_3), 1.32–1.44 (2H, m, $CH_2CH(CH_3)_2$), 1.58–68 (1H, m, $CH_2CH(CH_3)_2$), 2.10–2.20 (1H, m, $CH(CH_3)_2$), 3.44–3.55 (2H, m, CH_2OH), 3.96–4.06 (1H, m, $CHCH_2CH(CH_3)_2$), 4.34–4.42 (1H, m, $CHCH(CH_3)_2$), 6.54–6.58 (1H, m, $CHCHCH$), 7.16 (1H, d, $J=3.4$ Hz, $CHCHCH$), 7.65 (1H, m, $CHCHCH$), 7.95 (1H, d, $J=8.8$ Hz, NH), 7.99 (1H, d, $J=8.3$ Hz, NH); ^{13}C NMR (75 MHz, CD_3OD) 17.8 (CH_3), 18.6 (CH_3), 21.1 (CH_3), 22.5 (CH_3), 24.6 ($CHCH_2CH(CH_3)_2$), 30.8 ($CHCH(CH_3)_2$), 39.7 ($CHCH_2CH(CH_3)_2$), 49.5 ($CHCH_2CH(CH_3)_2$), 59.0 (CH_2OH), 64.3 ($CHCH(CH_3)_2$), 111.8 ($CHCHCH$), 114.4, ($CHCHCH$), 145.1 ($CHCHCH$), 147.2 (CO), 159.0 (CONH), 172.0 (CONH); m/z (ES) 311 [$M+(H)^+$], 100%; 333 [$M+(Na)^+$], 20%.

4.1.1.2. Thiophene-2-carboxylic acid [(S)-1-((S)-1-hydroxymethyl-3-methyl-butylcarbamoyl)-2-methyl-propyl]-amide (17). Reaction of **15** (as prepared above) with 2-thiophene-carbonyl chloride according to general procedure A gave **17** as a colourless

crystalline solid (0.7 g, 56%). Mp 181–183 °C; HRMS (ES^+) calcd for $\text{C}_{16}\text{H}_{27}\text{N}_2\text{O}_3\text{S}$ ($\text{M}+\text{H}^+$) 327.1742 found 327.1758; ^1H NMR (500 MHz, CDCl_3) 0.86 (6H, d, $J = 7.0$ Hz, $2 \times \text{CH}_3$), 1.03 (3H, d, $J = 7.0$ Hz, CH_3), 1.04 (3H, d, $J = 7.0$ Hz, CH_3), 1.30–1.44 (2H, m, $\text{CH}_2\text{CH}(\text{CH}_3)_2$), 1.54–1.64 (1H, m, $\text{CH}_2\text{CH}(\text{CH}_3)_2$), 2.21 (1H, sextet, $J = 7.0$ Hz, $\text{CH}(\text{CH}_3)_2$), 2.80 (1H, br s, OH), 3.54–3.62 (1H, m, CH_2OH), 3.66–3.74 (1H, m, CH_2OH), 4.00–4.10 (1H, m, $\text{CHCH}_2\text{CH}(\text{CH}_3)_2$), 4.45 (1H, app t, $J = 8.0$ Hz, $\text{CHCH}(\text{CH}_3)_2$), 6.68 (1H, d, $J = 8.0$ Hz, NH), 6.91 (1H, d, $J = 8.0$ Hz, NH), 7.08 (1H, t, $J = 4.0$ Hz, CHCHCH), 7.50 (1H, d, $J = 5.0$ Hz, SCHCHCH), 7.61 (1H, d, $J = 3.0$ Hz, CHCHCH); ^{13}C NMR (75 MHz, CDCl_3) 18.8 (CH_3), 19.2 (CH_3), 22.2 (CH_3), 22.7 (CH_3), 24.7 ($\text{CHCH}_2\text{CH}(\text{CH}_3)_2$), 31.1 ($\text{CHCH}(\text{CH}_3)_2$), 39.6 ($\text{CHCH}_2\text{CH}(\text{CH}_3)_2$), 50.5 ($\text{CHCH}_2\text{CH}(\text{CH}_3)_2$), 59.6 (CH_2OH), 66.0 ($\text{CHCH}(\text{CH}_3)_2$), 127.5 (CHCHCH), 128.4 (CHCHCH), 130.4 (CHCHCH), 138.5 (CS), 162.1 (CONH), 172.3 (CONH); m/z (ES) 327 [$\text{M}+(\text{H})$] $^+$, 100%; 349 [$\text{M}+(\text{Na})$] $^+$, 90%. Anal. Calcd for $\text{C}_{16}\text{H}_{26}\text{N}_2\text{O}_3\text{S}$: C, 58.87; H, 8.03; N, 8.58. Found C, 58.74; H, 8.05; N, 8.56.

4.1.2. General procedure B: amide bond formation

To a solution of *N,N*-dimethylformamide were added the amine (1.2 equiv), the carboxylic acid (1.0 equiv), HATU (1.0 equiv) and DIPEA (2.5 equiv). The solution was stirred at rt overnight then diluted with ethyl acetate and washed with water and brine. The organic phase was separated, dried over MgSO_4 and concentrated in vacuo.

4.1.2.1. 1*H*-Pyrrole-2-carboxylic acid [(*S*)-1-((*S*)-1-hydroxymethyl-3-methyl-butylcarbamoyl)-2-methyl-propyl]-amide (18).

Reaction of **15** (as prepared above) with 1*H*-pyrrole-2-carboxylic acid according to general procedure **B** gave **18** as an orange solid (0.26 g, 84%). Mp 110–112 °C; HRMS (ES^+) calcd for $\text{C}_{16}\text{H}_{28}\text{N}_3\text{O}_3$ ($\text{M}+\text{H}^+$) 310.2131 found 310.2134; ^1H NMR (500 MHz, CD_3OD) 0.86 (3H, d, $J = 7.0$ Hz, CH_3), 0.89 (3H, d, $J = 7.0$ Hz, CH_3), 0.97–1.00 (6H, m, $2 \times \text{CH}_3$), 1.35–1.40 (2H, m, $\text{CH}_2\text{CH}(\text{CH}_3)_2$), 1.55–1.59 (1H, m, $\text{CH}_2\text{CH}(\text{CH}_3)_2$), 2.11–2.12 (1H, m, $\text{CH}(\text{CH}_3)_2$), 3.43–3.48 (2H, m, CH_2OH), 3.98–4.02 (1H, m, $\text{CHCH}_2\text{CH}(\text{CH}_3)_2$), 4.26 (1H, dd, $J = 9.0$ Hz, $J = 2.0$ Hz, $\text{CHCH}(\text{CH}_3)_2$), 6.16–6.17 (1H, m, CHCHCH), 6.86–6.87 (1H, m, CHCHCH), 6.91–6.92 (1H, m, CHCHCH), 7.60 (1H, d, $J = 9.0$ Hz, NH), 7.85 (1H, d, $J = 9.0$ Hz, NH); ^{13}C NMR (75 MHz, CD_3OD) 19.4 (CH_3), 20.2 (CH_3), 22.6 (CH_3), 24.0 (CH_3), 26.1 ($\text{CHCH}_2\text{CH}(\text{CH}_3)_2$), 31.9 ($\text{CHCH}(\text{CH}_3)_2$), 41.3 ($\text{CHCH}_2\text{CH}(\text{CH}_3)_2$), 51.0 ($\text{CHCH}_2\text{CH}(\text{CH}_3)_2$), 60.6 (CH_2OH), 65.8 ($\text{CHCH}(\text{CH}_3)_2$), 110.6 (CHCHCH), 112.8 (CHCHCH), 123.5 (CHCHCH), 126.7 (CN), 163.6 (CONH), 174.2 (CONH); m/z (ES) 310 [$\text{M}+(\text{H})$] $^+$, 100%; 332 [$\text{M}+(\text{Na})$] $^+$, 30%. Anal. Calcd for $\text{C}_{16}\text{H}_{27}\text{N}_3\text{O}_3$: C, 62.11; H, 8.80; N, 13.58. Found C, 61.89; H, 8.44; N, 13.70.

4.1.2.2. 5-Formyl-furan-2-carboxylic acid [(*S*)-1-((*S*)-1-hydroxymethyl-3-methyl-butylcarbamoyl)-2-methyl-propyl]-amide (19).

Reaction of **15** (as prepared above) with (5-formyl)-furan-2-carboxylic acid according to general procedure **B** gave **19** as white solid (180 mg, 30%). Mp 46–48 °C; HRMS (ES^+) calcd for $\text{C}_{17}\text{H}_{26}\text{N}_2\text{O}_5$ ($\text{M}+\text{H}^+$) 339.1906 found 339.1920; ^1H NMR (500 MHz, CDCl_3) 0.89 (6H, m, $2 \times \text{CH}_3$), 1.04 (6H, m, $2 \times \text{CH}_3$), 1.37–1.43 (2H, m, $\text{CH}_2\text{CH}(\text{CH}_3)_2$), 1.62 (1H, m, $\text{CH}_2\text{CH}(\text{CH}_3)_2$), 2.17–2.26 (1H, m, $\text{CH}(\text{CH}_3)_2$), 3.60 (1H, dd, $J = 5.5$ Hz, $J = 11.0$ Hz, CH_2OH), 3.71 (1H, dd, $J = 3.4$ Hz, $J = 11.0$ Hz, CH_2OH), 4.05–4.10 (1H, m, CHCH_2OH), 4.38–4.41 (1H, m, $\text{CHCH}(\text{CH}_3)_2$), 6.21 (1H, d, $J = 8.0$ Hz, NH), 7.28 (2H, m, CHCH and CHCH), 9.75 (1H, s, CHO); ^{13}C NMR (75 MHz, CDCl_3) 18.5 (CH_3), 19.1 (CH_3), 22.2 (CH_3), 22.7 (CH_3), 24.7 ($\text{CHCH}_2\text{CH}(\text{CH}_3)_2$), 31.4 ($\text{CHCH}(\text{CH}_3)_2$), 39.7 ($\text{CHCH}_2\text{CH}(\text{CH}_3)_2$), 49.8 ($\text{CHCH}_2\text{CH}(\text{CH}_3)_2$), 58.7 (CH_2OH), 65.0 ($\text{CHCH}(\text{CH}_3)_2$), 115.9 (CHCH), 121.4 (CHCCHO), 150.6 (C(=O)NH), 152.5 (CO), 157.3 (CONH), 170.9 (CONH), 178.5 (CCHO); m/z (ES) 339 [$\text{M}+(\text{H})$] $^+$, 100%. Anal. Calcd for $\text{C}_{17}\text{H}_{26}\text{N}_2\text{O}_5$: C, 60.34; H, 7.74; N, 8.28. Found C, 60.58; H, 7.57; N, 8.09.

4.1.2.3. 5-Formyl-thiophene-2-carboxylic acid [(*S*)-1-((*S*)-1-hydroxymethyl-3-methyl-butylcarbamoyl)-2-methyl-propyl]-amide (20).

Reaction of **15** (as prepared above) with (5-formyl)-thiophene-2-carboxylic acid according to general procedure **B** gave **20** as a yellow solid (1.2 g, 88%). Mp 133–135 °C; HRMS (ES^+) calcd for $\text{C}_{17}\text{H}_{27}\text{N}_2\text{O}_4\text{S}$ ($\text{M}+\text{H}^+$) 355.1692 found 355.1695; ^1H NMR (500 MHz, CDCl_3) 0.88 (6H, m, $2 \times \text{CH}_3$), 0.88 (3H, d, $J = 6.3$ Hz, CH_3), 1.03 (3H, d, $J = 5.1$ Hz, CH_3), 1.04 (3H, d, $J = 6.1$ Hz, CH_3), 1.32–1.46 (2H, m, $\text{CH}_2\text{CH}(\text{CH}_3)_2$), 1.56–1.66 (1H, m, $\text{CH}_2\text{CH}(\text{CH}_3)_2$), 2.16–2.26 (1H, m, $\text{CH}(\text{CH}_3)_2$), 2.94–3.14 (1H, m, OH), 3.60 (1H, dd, $J = 11.0$ Hz, $J = 5.7$ Hz, CH_2OH), 3.70 (1H, dd, $J = 11.0$ Hz, $J = 3.7$ Hz, CH_2OH), 4.02–4.11 (1H, m, CHCH_2OH), 4.41 (1H, app t, $J = 8.4$ Hz, $\text{CHCH}(\text{CH}_3)_2$), 6.4 (1H, d, $J = 8.1$ Hz, NH), 7.16 (1H, d, $J = 8.4$ Hz, NH), 7.60 (1H, d, $J = 4.0$ Hz, CHCH), 7.73 (1H, d, $J = 4.0$ Hz, CHCH), 9.95 (1H, s, CHO); ^{13}C NMR (75 MHz, CDCl_3) 18.8 (CH_3), 19.2 (CH_3), 22.2 (CH_3), 22.8 (CH_3), 24.8 ($\text{CHCH}_2\text{CH}(\text{CH}_3)_2$), 31.0 ($\text{CHCH}(\text{CH}_3)_2$), 39.7 ($\text{CHCH}_2\text{CH}(\text{CH}_3)_2$), 50.5 (CH_2OH), 59.9 ($\text{CHCH}_2\text{CH}(\text{CH}_3)_2$), 65.8 ($\text{CHCH}(\text{CH}_3)_2$), 128.7 (CHCH), 128.7 (CHCCHO), 135.5 (C(=O)NH), 146.4 (CS), 161.2 (CONH), 171.8 (CONH), 183.2 (CCHO); m/z (ES) 355 [$\text{M}+(\text{H})$] $^+$, 100%; 377 [$\text{M}+(\text{Na})$] $^+$, 50%. Anal. Calcd for $\text{C}_{17}\text{H}_{26}\text{N}_2\text{O}_4\text{S}$: C, 57.60; H, 7.39; N, 7.90. Found C, 57.34; H, 7.69; N, 8.10.

4.1.2.4. 5-Formyl-pyrrole-2-carboxylic acid [(*S*)-1-((*S*)-1-hydroxymethyl-3-methyl-butylcarbamoyl)-2-methyl-propyl]-amide (25).

Reaction of **15** (as prepared above) with (5-formyl)-1*H*-pyrrole-2-carboxylic acid **23** according to general procedure **B** gave **25** as a yellow solid (0.5 g, 39%). Mp 102–104 °C; HRMS (ES^+) calcd for $\text{C}_{17}\text{H}_{27}\text{N}_3\text{O}_4$ ($\text{M}+\text{H}^+$) 338.2080 found 338.2086; ^1H NMR (500 MHz, CDCl_3) 0.80 (3H, d, $J = 6.3$ Hz, CH_3), 0.82 (3H, d, $J = 6.3$ Hz, CH_3), 1.02 (3H, d, $J = 6.8$ Hz, CH_3), 1.05 (3H, d, $J = 6.8$ Hz, CH_3), 1.35–1.37 (2H, m, $\text{CH}_2\text{CH}(\text{CH}_3)_2$), 1.51–1.58 (1H, m, $\text{CH}_2\text{CH}(\text{CH}_3)_2$), 2.09–2.16 (1H, m, $\text{CH}(\text{CH}_3)_2$), 3.80–3.89 (2H, m, CH_2OH), 4.17–4.20 (1H, m, $\text{CHCH}_2\text{CH}(\text{CH}_3)_2$), 5.01 (1H, app t, $J = 15.0$ Hz, $\text{CHCH}(\text{CH}_3)_2$), 6.78–6.80 (1H, m, CHCH), 6.97–6.99 (1H, m, CHCCHO), 7.23 (1H, d, $J = 16.0$ Hz, NH), 8.17 (1H, d, $J = 16.0$ Hz, NH), 9.53 (1H, s, CHO), 11.78 (1H, br s, NH); ^{13}C NMR (75 MHz, CDCl_3) 18.9 (CH_3), 19.1 (CH_3), 22.4 (CH_3), 22.8 (CH_3), 24.9 ($\text{CHCH}_2\text{CH}(\text{CH}_3)_2$), 32.2 ($\text{CHCH}(\text{CH}_3)_2$), 40.0 ($\text{CHCH}_2\text{CH}(\text{CH}_3)_2$), 48.6 ($\text{CHCH}_2\text{CH}(\text{CH}_3)_2$), 58.4 (CH_2OH), 64.8 ($\text{CHCH}(\text{CH}_3)_2$), 110.7 (CHCH), 122.0, (CHCCHO), 132.3 (C(=O)NH), 133.6 (CN), 159.5 (CONH), 171.0 (CONH), 181.0 (CCHO); m/z (ES) 338 [$\text{M}+(\text{H})$] $^+$, 30%; 360 [$\text{M}+(\text{Na})$] $^+$, 100%. Anal. Calcd for $\text{C}_{17}\text{H}_{27}\text{N}_3\text{O}_4$: C, 60.51; H, 8.07; N, 12.45. Found C, 60.57; H, 8.01; N, 12.57.

4.1.2.5. 4-Formyl-1*H*-pyrrole-2-carboxylic acid [(*S*)-1-((*S*)-1-hydroxymethyl-3-methyl-butylcarbamoyl)-2-methyl-propyl]-amide (26).

Reaction of **15** (as prepared above) with (4-formyl)-1*H*-pyrrole-2-carboxylic acid **24** according to general procedure **B** gave **26** as a pale yellow glassy solid (0.1 g, 36%). Mp 112–115 °C; HRMS (ES^+) calcd for $\text{C}_{17}\text{H}_{27}\text{N}_3\text{O}_4$ ($\text{M}+\text{H}^+$) 338.2080 found 338.2066; ^1H NMR (500 MHz, CD_3OD) 0.86 (3H, d, $J = 6.8$ Hz, CH_3), 0.89 (3H, d, $J = 6.8$ Hz, CH_3), 0.98–1.02 (6H, m, $2 \times \text{CH}_3$), 1.00 (3H, d, $J = 5.0$ Hz, CH_3), 1.32–1.44 (2H, m, $\text{CH}_2\text{CH}(\text{CH}_3)_2$), 1.60–1.68 (1H, m, $\text{CH}_2\text{CH}(\text{CH}_3)_2$), 2.08–2.13 (1H, m, $\text{CH}(\text{CH}_3)_2$), 3.42–3.52 (2H, m, CH_2OH), 3.96–4.02 (1H, m, $\text{CHCH}_2\text{CH}(\text{CH}_3)_2$), 4.22–4.28 (1H, m, $\text{CHCH}(\text{CH}_3)_2$), 6.84–6.88 (1H, m, $\text{CHC}(\text{CHO})$), 6.92–6.96 (1H, m, CHNH), 7.64–7.68 (1H, m, NH), 7.82–8.00 (1H, m, NH) 9.73 (1H, s, CHO); ^{13}C NMR (75 MHz, $(\text{CD}_3)_2\text{SO}$) 19.5 (CH_3), 20.0 (CH_3), 22.5 (CH_3), 24.1 (CH_3), 24.8 ($\text{CHCH}_2\text{CH}(\text{CH}_3)_2$), 32.2 ($\text{CHCH}(\text{CH}_3)_2$), 41.1 ($\text{CHCH}_2\text{CH}(\text{CH}_3)_2$), 49.4 ($\text{CHCH}_2\text{CH}(\text{CH}_3)_2$), 59.3 (CH_2OH), 64.6 ($\text{CHCH}(\text{CH}_3)_2$), 109.5 (CHCH), 127.1, (CHCCHO), 129.2 (C(=O)NH), 130.9 (CN), 160.6 (CONH), 171.3 (CONH), 186.6 (CCHO); m/z (ES) 338 [$\text{M}+(\text{H})$] $^+$, 10%; 360 [$\text{M}+(\text{Na})$] $^+$, 100%. Anal. Calcd for $\text{C}_{17}\text{H}_{27}\text{N}_3\text{O}_4$: C, 60.51; H, 8.07; N, 12.45. Found C, 60.12; H, 8.01; N, 12.44.

4.1.2.6. 5-Formyl-1-methyl-1H-pyrrole-2-carboxylic acid [(S)-1-((S)-1-hydroxymethyl-3-methylbutylcarbamoyl)-2-methyl-propyl]-amide (30). Reaction of **15** (as prepared above) with (5-formyl)-1-methyl-1H-pyrrole-2-carboxylic acid **27** according to general procedure **B** gave **30** as an orange solid (0.32 g, 56%). Mp 178–180 °C; HRMS (ES⁺) calcd for C₁₈H₃₀N₃O₄ (M+H⁺) 352.2236 found 352.2245; ¹H NMR (500 MHz, CD₃OD) 0.88–0.93 (6H, m, 2 × CH₃), 1.00–1.05 (6H, m, 2 × CH₃), 1.32–1.46 (2H, m, CH₂CH(CH₃)₂), 1.58–1.66 (1H, m, CH₂CH(CH₃)₂), 2.14–2.24 (1H, m, CH(CH₃)₂), 3.54–3.62 (1H, m, CH₂OH), 3.67–3.74 (1H, m, CH₂OH), 4.03–4.11 (1H, m, CHCH₂CH(CH₃)₂), 4.21 (3H, s, NCH₃), 4.32 (1H, dd, *J* = 7.2 Hz, *J* = 8.4 Hz, CHCH(CH₃)₂), 6.09 (1H, d, *J* = 7.9 Hz, NH), 6.63 (1H, d, *J* = 4.4 Hz, CHCH), 6.76 (1H, d, *J* = 8.4 Hz, NH), 6.88 (1H, d, *J* = 4.4 Hz, CHCH), 9.69 (1H, s, CHO); ¹³C NMR (75 MHz, CDCl₃) 18.7 (CH₃), 19.5 (CH₃), 21.4 (CH₃), 23.2 (CH₃), 25.1 (CHCH₂CH(CH₃)₂), 31.5 (CHCH(CH₃)₂), 34.8 (CHCH₂CH(CH₃)₂), 40.2 (CH₂OH), 50.5 (CHCH₂CH(CH₃)₂), 59.3 (CHCH(CH₃)₂), 66.0 (NCH₃), 112.2 (CHCH), 122.6 (CHCCHO), 133.6 (CCONH), 135.0 (CNCH₃), 161.5 (CONH), 171.6 (CONH), 181.3 (CCHO); *m/z* (ES) 352 [M+(H)]⁺, 100%. Anal. Calcd for C₁₈H₂₉N₃O₄: C, 60.52; H, 8.32; N, 11.96. Found C, 60.46; H, 8.21; N, 11.69.

4.1.2.7. 5-Methyl-1H-pyrrole-2-carboxylic acid [(S)-1-((S)-1-hydroxymethyl-3-methyl-butylcarbamoyl)-2-methyl-propyl]-amide (31). Reaction of **15** (as prepared above) with (5-methyl)-1H-pyrrole-2-carboxylic acid **28** according to general procedure **B** gave **31** as a white solid (0.27 g, 29%). Mp 173–175 °C; HRMS (ES⁺) calcd for C₁₇H₃₀N₃O₃ (M+H⁺) 324.2287 found 352.2286; ¹H NMR (500 MHz, CD₃OD) 0.86 (3H, d, *J* = 6.5 Hz, CH₃), 0.88 (3H, d, *J* = 6.5 Hz, CH₃), 0.103 (3H, d, *J* = 6.5 Hz, CH₃), 1.04 (3H, d, *J* = 6.5 Hz, CH₃), 1.26–1.42 (2H, m, CH₂CH(CH₃)₂), 1.50–1.62 (1H, m, CH₂CH(CH₃)₂), 2.12–2.22 (1H, m, CH(CH₃)₂), 2.28 (3H, s, CCH₃), 3.61 (1H, dd, *J* = 11.2 Hz, *J* = 4.8 Hz, CH₂OH), 3.74 (1H, dd, *J* = 11.2 Hz, *J* = 2.9 Hz, CH₂OH), 4.04–4.12 (1H, m, CHCH₂CH(CH₃)₂), 4.50 (1H, app t, *J* = 8.4 Hz, CHCH(CH₃)₂), 5.92 (1H, br s, CHCH), 6.65 (1H, br s, CHCH), 6.71 (1H, br s, NH), 7.35 (1H, br s, NH), 9.92 (1H, s, CHO); ¹³C NMR (75 MHz, CD₃OD) 16.8 (CH₃), 18.0 (CH₃), 20.2 (CH₃), 22.4 (CH₃), 23.6 (CHCH₂CH(CH₃)₂), 30.0 (CHCH(CH₃)₂), 36.8 (CHCH₂CH(CH₃)₂), 49.2 (CHCH₂CH(CH₃)₂), 60.5 (CH₂OH), 65.8 (CHCH(CH₃)₂), 105.3 (CH₃), 126.9 (CHCH), 127.5 (CHCH), 135.9 (CCH₃), 156.3 (CONH), 171.6 (CONH); *m/z* (ES) 324 [M+(H)]⁺, 100%; 346 [M+(Na)]⁺, 50%. Anal. Calcd for C₁₇H₂₉N₃O₃: C, 63.13; H, 9.04; N, 12.99. Found C, 62.85; H, 9.16; N, 12.89.

4.1.2.8. 5-[(S)-1-((S)-1-Hydroxymethyl-3-methyl-butylcarbamoyl)-2-methyl-propylcarbamoyl]-1H-pyrrole-2-carboxylic acid methyl ester (32). Reaction of **15** (as prepared above) with 1H-Pyrrole-2,5-dicarboxylic acid monomethyl ester **29** according to general procedure **B** gave **32** as a white solid (0.42 g, 64%). Mp 115–117 °C; HRMS (ES⁺) calcd for C₁₈H₃₀N₃O₅ (M+H⁺) 368.2185 found 368.2185; ¹H NMR (500 MHz, CDCl₃) 0.85 (3H, d, *J* = 7.0 Hz, CH₃), 0.89 (3H, d, *J* = 7.0 Hz, CH₃), 0.95 (3H, d, *J* = 7.0 Hz, CH₃), 1.00 (3H, d, *J* = 7.0 Hz, CH₃), 1.38–1.40 (1H, m, CH₂CH(CH₃)₂), 1.41–1.58 (2H, m, CH₂CH(CH₃)₂), 2.16–2.17 (1H, m, CH(CH₃)₂), 3.80–3.84 (2H, m, CH₂OH), 3.87 (1H, s, OCH₃), 4.17–4.19 (1H, m, CHCH₂CH(CH₃)₂), 4.94 (1H, app t, *J* = 9.0 Hz, CHCH(CH₃)₂), 6.73 (1H, s, CHCH), 6.86–6.88 (1H, m, CHCCOMe), 7.17 (1H, d, *J* = 9.0 Hz, NH), 8.24 (1H, d, *J* = 8.5 Hz, NH); ¹³C NMR (75 MHz, CDCl₃) 18.6 (CH₃), 19.5 (CH₃), 22.9 (CH₃), 23.0 (CH₃), 25.2 (CHCH₂CH(CH₃)₂), 31.8 (CHCH(CH₃)₂), 34.8 (CHCH₂CH(CH₃)₂), 49.2 (CH₂OH), 52.1 (CHCH₂CH(CH₃)₂), 59.2 (CHCH(CH₃)₂), 65.4 (OCH₃), 111.2 (CHCH), 116.3 (CHCCHO), 125.0 (CCONH), 130.4 (CCO₂Me), 160.2 (CONH), 162.3 (CONH), 172.2 (CCO₂Me); *m/z* (ES) 368 [M+(H)]⁺, 100%. Anal. Calcd for C₁₈H₂₉N₃O₅: C, 58.84; H, 7.96; N, 11.44. Found C, 58.62; H, 7.98; N, 11.43.

4.1.3. General procedure C: oxidation

A solution of the alcohol (1.0 equiv) in a 1:3 mixture of dimethylsulfoxide and dichloromethane was cooled over an ice bath, followed by the addition of DIPEA (4.3 equiv). To this ice-cold reaction mixture, a solution of SO₃·Pyr complex (4.5 equiv) dissolved in dimethylsulfoxide was added. The reaction mixture was maintained at a low temperature for a further 2 h (or until TLC indicated complete consumption of the starting alcohol). The reaction mixture was diluted with ethyl acetate and partitioned between ethyl acetate and 1 M HCl. The organic phase was washed with saturated aqueous sodium bicarbonate and brine, then dried over MgSO₄ and concentrated in vacuo.

4.1.3.1. Furan-2-carboxylic acid [(S)-1-((S)-1-formyl-3-methyl-butylcarbamoyl)-2-methyl-propyl]-amide (4). Oxidation of **16** according to general procedure C gave **4** as a colourless oil (0.10 g, 58%). HRMS (ES⁺) calcd for C₁₆H₂₅N₂O₄ (M+H⁺) 309.1820 found 309.1814; *v*_{max} (KBr) 1738 (CHO); ¹H NMR (500 MHz, CDCl₃) 0.80 (3H, d, *J* = 5.6 Hz, CH₃), 0.83 (3H, d, *J* = 5.6 Hz, CH₃), 1.00 (3H, d, *J* = 6.4 Hz, CH₃), 1.04 (3H, d, *J* = 6.4 Hz, CH₃), 1.34–1.44 (1H, m, CH₂CH(CH₃)₂), 1.56–1.66 (2H, m, CH₂CH(CH₃)₂), 2.15–2.24 (1H, m, CH(CH₃)₂), 4.40–4.48 (1H, m, CHCH₂CH(CH₃)₂), 4.71 (1H, dd, *J* = 9.1 Hz, *J* = 7.1 Hz, CHCH(CH₃)₂), 6.46 (1H, m, CHCHCH), 7.07 (1H, d, *J* = 3.6 Hz, CHCHCH), 7.19 (1H, d, *J* = 9.1 Hz, NH), 7.43 (1H, s, CHCHCH), 7.63 (1H, d, *J* = 7.4 Hz, NH), 9.56 (1H, s, CHO); ¹³C NMR (75 MHz, CDCl₃) 18.2 (CH₃), 19.2 (CH₃), 21.7 (CH₃), 22.8 (CH₃), 24.6 (CHCH₂CH(CH₃)₂), 31.6 (CHCH(CH₃)₂), 37.1 (CHCH₂CH(CH₃)₂), 57.2 (CHCH₂CH(CH₃)₂), 57.7 (CHCH(CH₃)₂), 112.0 (CHCHCH), 114.7, (CHCHCH), 144.4 (CHCHCH), 147.2 (CO), 158.2 (CONH), 171.6 (CONH), 199.6 (CHO); *m/z* (ES) 310 [M+(H)]⁺, 100%; 332 [M+(Na)]⁺, 20%.

4.1.3.2. Thiophene-2-carboxylic acid [(S)-1-((S)-1-formyl-3-methyl-butylcarbamoyl)-2-methyl-propyl]-amide (5). Oxidation of **17** according to general procedure C gave **5** as a colourless crystalline solid (0.13 g, 51%). Mp 178–180 °C; HRMS (ES⁺) calcd for C₁₆H₂₅N₂O₃S (M+H⁺) 325.1586 found 325.1578; *v*_{max} (KBr) 1736 (CHO); ¹H NMR (500 MHz, CD₃OD) 0.87 (3H, d, *J* = 4.5 Hz, CH₃), 0.89 (3H, d, *J* = 4.0 Hz, CH₃), 1.02 (3H, d, *J* = 11.5 Hz, CH₃), 1.06 (3H, d, *J* = 7.0 Hz, CH₃), 1.43–1.50 (2H, m, CH₂CH(CH₃)₂), 1.65–1.72 (1H, m, CH₂CH(CH₃)₂), 2.20–2.26 (1H, m, CH(CH₃)₂), 4.45–4.49 (1H, m, CHCH(CH₃)₂), 4.62 (1H, dd, *J* = 7.5 Hz, *J* = 8.0 Hz, CHCH₂CH(CH₃)₂), 6.97 (1H, d, *J* = 9.0 Hz, CHCHCH), 7.07 (1H, dd, *J* = 4.5 Hz, *J* = 3.5 Hz, CHCHCH), 7.12–7.16 (1H, m, CHCHCH), 7.50 (1H, d, *J* = 6.0 Hz, NH), 7.62 (1H, d, *J* = 5.0 Hz, NH), 9.57 (CHO); ¹³C NMR (75 MHz, CDCl₃) 18.5 (CH₃), 19.3 (CH₃), 21.8 (CH₃), 22.9 (CH₃), 24.7 (CHCH₂CH(CH₃)₂), 31.4 (CHCH(CH₃)₂), 37.4 (CHCH₂CH(CH₃)₂), 57.5 (CHCH₂CH(CH₃)₂), 58.7 (CHCH(CH₃)₂), 127.8 (CHCHCH), 128.5, (CHCHCH), 130.5 (CHCHCH), 138.3 (CS), 162.0 (CONH), 171.8 (CONH), 200.20 (CHO); *m/z* (ES) 325 [M+(H)]⁺, 100%; 345 [M+(Na)]⁺, 20%. Anal. Calcd for C₁₆H₂₄N₂O₃S: C, 59.23; H, 7.46; N, 8.63. Found C, 59.32; H, 7.59; N, 8.61.

4.1.3.3. 1H-Pyrrole-2-carboxylic acid [(S)-1-((S)-1-formyl-3-methyl-butylcarbamoyl)-2-methyl-propyl]-amide (6). Oxidation of **18** according to general procedure C gave **6** as a colourless crystalline solid (0.20 g, 71%). Mp 165–167 °C; HRMS (ES⁺) calcd for C₁₆H₂₆N₃O₃ (M+H⁺) 308.1974 found 308.1961; *v*_{max} (KBr) 1741 (CHO); ¹H NMR (500 MHz, CD₃OD) 0.79 (3H, d, *J* = 10.5 Hz, CH₃), 0.81 (3H, d, *J* = 11.5 Hz, CH₃), 0.87 (3H, d, *J* = 12.0 Hz, CH₃), 0.89 (3H, d, *J* = 12.0 Hz, CH₃), 1.33–1.38 (2H, m, CH₂CH(CH₃)₂), 1.53–1.56 (1H, m, CH₂CH(CH₃)₂), 2.10–2.15 (1H, m, CH(CH₃)₂), 4.02–4.07 (1H, m, CHCH₂CH(CH₃)₂), 4.30 (1H, m, CHCH(CH₃)₂), 6.03–6.05 (1H, m, CHCHCH), 6.83–6.85 (1H, m, CHCHCH), 6.85–6.87 (1H, m, CHCHCH) 7.92 (1H, d, *J* = 9.0 Hz, NH), 8.40 (1H, d, *J* = 9.0 Hz, NH), 9.36 (1H, s, CHO), 11.45 (1H, s, NH); ¹³C NMR

(75 MHz, $(\text{CD}_3)_2\text{SO}$) 18.7 (CH_3), 18.8 (CH_3), 19.4 (CH_3), 21.4 (CH_3), 23.2 ($\text{CHCH}_2\text{CH}(\text{CH}_3)_2$), 30.3 ($\text{CHCH}(\text{CH}_3)_2$), 36.4 ($\text{CHCH}_2\text{CH}(\text{CH}_3)_2$), 56.8 ($\text{CHCH}_2\text{CH}(\text{CH}_3)_2$), 57.9 ($\text{CHCH}(\text{CH}_3)_2$), 108.7 (CHCHCH), 111.2, (CHCHCH), 121.6 (CHCHCH), 125.9 (CN), 160.5 (CONH), 172.0 (CONH), 201.3 (CHO); m/z (ES) 308 $[\text{M}+(\text{H})]^+$, 100%. Anal. Calcd for $\text{C}_{16}\text{H}_{25}\text{N}_3\text{O}_3$: C, 62.52; H, 8.20; N, 13.67. Found C, 62.66; H, 8.36; N, 13.59.

4.1.3.4. 5-Formyl-furan-2-carboxylic acid [(S)-1-((S)-1-formyl-3-methyl-butylcarbamoyl)-2-methyl-propyl]-amide (7). Oxidation of **19** according to general procedure C gave **7** as a colourless oil (100 mg, 80%). HRMS (ES^+) calcd for $\text{C}_{17}\text{H}_{25}\text{N}_2\text{O}_5$ ($\text{M}+\text{H}^+$) 337.1740 found 337.1763; v_{max} (KBr) 1734 (CHO); ^1H NMR (500 MHz, CDCl_3); 0.87–0.94 (6H, m, $2\times \text{CH}_3$), 1.03 (3H, d, $J = 6.7$ Hz, CH_3), 1.04 (3H, d, $J = 6.7$ Hz, CH_3), 1.40–1.49 (1H, m, $\text{CH}_2\text{CH}(\text{CH}_3)_2$), 1.64–1.74 (1H, m, $\text{CH}_2\text{CH}(\text{CH}_3)_2$), 2.18–2.28 (1H, m, $\text{CH}(\text{CH}_3)_2$), 4.54–4.62 (2H, m, $\text{CHCH}(\text{CH}_3)_2$ and CHCHO), 6.85 (1H, d, $J = 7.1$ Hz, NH), 7.20–7.32 (2H, m, CHCH and CHCH), 7.36 (1H, d, $J = 9.1$ Hz, NH), 9.59 (1H, s, CHCHO), 9.73 (1H, s, CCHO); ^{13}C NMR (75 MHz, CD_3OD) 18.4 (CH_3), 19.3 (CH_3), 21.8 (CH_3), 22.9 (CH_3), 24.7 ($\text{CHCH}_2\text{CH}(\text{CH}_3)_2$), 31.4 ($\text{CHCH}(\text{CH}_3)_2$), 37.3 ($\text{CHCH}_2\text{CH}(\text{CH}_3)_2$), 57.4 ($\text{CHCH}_2\text{CH}(\text{CH}_3)_2$), 58.4 ($\text{CHCH}(\text{CH}_3)_2$), 116.0 (CHCH), 121.1 (CHCCHO), 150.5 (CCONH), 152.6 (CO), 157.4 (CONH), 171.2 (CONH), 178.5 (CCHO), 199.6 (CHCHO); m/z (ES) 337 $[\text{M}+\text{H}]^+$, 100%.

4.1.3.5. 5-Formyl-thiophene-2-carboxylic acid [(S)-1-((S)-1-formyl-3-methyl-butylcarbamoyl)-2-methyl-propyl]-amide (8). Oxidation of **20** according to general procedure C gave **8** as a yellow solid (0.47 g, 89%). Mp 162–164 °C; HRMS (ES^+) calcd for $\text{C}_{17}\text{H}_{25}\text{N}_2\text{O}_4\text{S}$ ($\text{M}+\text{H}^+$) 353.1535 found 353.1521; v_{max} (KBr) 1738 (CHO); ^1H NMR (500 MHz, CDCl_3) 0.88 (6H, m, $2\times \text{CH}_3$), 1.03 (3H, d, $J = 6.6$ Hz, CH_3), 1.08 (3H, d, $J = 6.6$ Hz, CH_3), 1.46–1.75 (2H, m, $\text{CH}_2\text{CH}(\text{CH}_3)_2$), 1.63–1.73 (1H, m, $\text{CH}_2\text{CH}(\text{CH}_3)_2$), 2.16–2.26 (1H, m, $\text{CH}(\text{CH}_3)_2$), 4.35–4.41 (1H, m, CHCHO), 4.66 (1H, app t, $J = 8.7$ Hz, $\text{CHCH}(\text{CH}_3)_2$), 7.71 (1H, d, $J = 4.0$ Hz, CHCH), 7.78 (1H, d, $J = 4.0$ Hz, CHCH), 7.82–7.90 (1H, m, NH), 8.19 (1H, d, $J = 8.4$ Hz, NH), 9.57 (1H, s, CHCHO), 9.95 (1H, s, CCHO); ^{13}C NMR (75 MHz, CDCl_3) 19.4 (CH_3), 19.5 (CH_3), 21.9 (CH_3), 23.2 (CH_3), 25.0 ($\text{CHCH}_2\text{CH}(\text{CH}_3)_2$), 31.0 ($\text{CHCH}(\text{CH}_3)_2$), 37.3 ($\text{CHCH}_2\text{CH}(\text{CH}_3)_2$), 60.1 ($\text{CHCH}_2\text{CH}(\text{CH}_3)_2$), 129.2 (CHCH), 135.9 (CHCCHO), 146.8 (CCONH), 146.8 (CS), 161.6 (CONH), 172.6 (CONH), 183.6 (CCHO), 199.4 (CHO); m/z (ES) 353 $[\text{M}+(\text{H})]^+$ 100%. Anal. Calcd for $\text{C}_{17}\text{H}_{24}\text{N}_2\text{O}_4\text{S}$: C, 57.93; H, 6.86; N, 7.95. Found C, 57.55; H, 6.80; N, 7.60.

4.1.3.6. 5-Formyl-pyrrole-2-carboxylic acid [(S)-1-((S)-1-formyl-3-methyl-butylcarbamoyl)-2-methyl-propyl]-amide (9). Oxidation of **25** according to general procedure C gave **9** as a yellow solid (0.2 g, 71%). Mp 70–72 °C; HRMS (ES^+) calcd for $\text{C}_{17}\text{H}_{25}\text{N}_3\text{O}_4$ ($\text{M}+\text{H}^+$) 336.1923 found 336.1925; v_{max} (KBr) 1738 (CHO); ^1H NMR (500 MHz, CDCl_3) 0.79 (3H, d, $J = 7.0$ Hz, CH_3), 0.82 (3H, d, $J = 7.0$ Hz, CH_3), 1.01 (3H, d, $J = 7.0$ Hz, CH_3), 1.06 (3H, d, $J = 7.0$ Hz, CH_3), 1.23–1.26 (1H, m, $\text{CH}_2\text{CH}(\text{CH}_3)_2$), 1.63–1.653 (2H, m, $\text{CH}_2\text{CH}(\text{CH}_3)_2$), 2.01–2.03 (1H, m, $\text{CH}(\text{CH}_3)_2$), 4.02–4.04 (1H, m, $\text{CHCH}_2\text{CH}(\text{CH}_3)_2$), 4.80 (1H, app t, $J = 8.0$ Hz, $\text{CHCH}(\text{CH}_3)_2$), 6.84–6.88 (1H, m, CHCH), 6.93–6.95 (1H, m, CHCCHO), 7.75 (1H, d, $J = 7.0$ Hz, NH), 7.82 (1H, d, $J = 7.0$ Hz, NH), 9.58 (1H, s, CHCHO), 9.60 (1H, s, CCHO), 11.82 (1H, br s, NH); ^{13}C NMR (75 MHz, CDCl_3) 18.9 (CH_3), 19.2 (CH_3), 21.63 (CH_3), 22.8 (CH_3), 24.6 ($\text{CHCH}_2\text{CH}(\text{CH}_3)_2$), 30.8 ($\text{CHCH}(\text{CH}_3)_2$), 37.2 ($\text{CHCH}_2\text{CH}(\text{CH}_3)_2$), 57.5 ($\text{CHCH}_2\text{CH}(\text{CH}_3)_2$), 59.1 ($\text{CHCH}(\text{CH}_3)_2$), 111.9 (CHCH), 121.1, (CHCCHO), 132.2 (CCONH), 134.2 (CN), 160.1 (CONH), 172.5 (CONH), 180.6 (CCHO), 199.5 (CHCHO); m/z (ES) 336 $[\text{M}+(\text{H})]^+$, 100%; 358 $[\text{M}+(\text{Na})]^+$, 10%. Anal. Calcd for $\text{C}_{17}\text{H}_{25}\text{N}_3\text{O}_4$: C, 60.88; H, 7.51; N, 12.53. Found C, 60.99; H, 7.28; N, 12.57.

4.1.3.7. 4-Formyl-1H-pyrrole-2-carboxylic acid [(S)-1-((S)-1-formyl-3-methyl-butylcarbamoyl)-2-methyl-propyl]-amide (10).

Oxidation of **26** according to general procedure C gave **10** as a colourless glassy solid (48 mg, 90%). Mp 101–103 °C; HRMS (ES^+) calcd for $\text{C}_{17}\text{H}_{25}\text{N}_3\text{O}_4$ ($\text{M}+\text{H}^+$) 336.1923 found 336.1922; v_{max} (KBr) 1736 (CHO); ^1H NMR (500 MHz, $(\text{CD}_3)_2\text{SO}$) 0.82 (3H, d, $J = 6.5$ Hz, CH_3), 0.86 (3H, d, $J = 6.0$ Hz, CH_3), 0.90 (3H, d, $J = 7.0$ Hz, CH_3), 1.06 (3H, d, $J = 7.5$ Hz, CH_3), 1.41–1.44 (1H, m, $\text{CH}_2\text{CH}(\text{CH}_3)_2$), 1.50–1.56 (1H, m, $\text{CH}_2\text{CH}(\text{CH}_3)_2$), 1.61–1.65 (1H, m, $\text{CH}_2\text{CH}(\text{CH}_3)_2$), 2.05–2.11 (1H, m, $\text{CH}(\text{CH}_3)_2$), 4.10–4.14 (1H, m, $\text{CHCH}_2\text{CH}(\text{CH}_3)_2$), 4.30 (1H, app t, $J = 8.5$ Hz, $\text{CHCH}(\text{CH}_3)_2$), 7.41 (1H, s, CHCH), 7.69 (1H, s, CHCCHO), 8.17 (1H, d, $J = 9.0$ Hz, NH), 8.42 (1H, d, $J = 7.5$ Hz, NH), 9.38 (1H, s, CHCHO), 9.72 (1H, s, CCHO), 12.30 (1H, br s, NH); ^{13}C NMR (75 MHz, $(\text{CD}_3)_2\text{SO}$) 18.7 (CH_3), 19.4 (CH_3), 21.6 (CH_3), 23.8 (CH_3), 24.1 ($\text{CHCH}_2\text{CH}(\text{CH}_3)_2$), 30.0 ($\text{CHCH}(\text{CH}_3)_2$), 36.2 ($\text{CHCH}_2\text{CH}(\text{CH}_3)_2$), 58.3 ($\text{CHCH}_2\text{CH}(\text{CH}_3)_2$), 59.8 ($\text{CHCH}(\text{CH}_3)_2$), 119.0 (CHCH), 126.5, (CHCCHO), 128.3 (CCONH), 130.3 (CN), 160.0 (CONH), 171.7 (CONH), 185.9 (CCHO) 201.2 (CHCHO); m/z (ES) 336 $[\text{M}+(\text{H})]^+$, 100%. Anal. Calcd for $\text{C}_{17}\text{H}_{25}\text{N}_3\text{O}_4$: C, 60.88; H, 7.51; N, 12.53. Found C, 60.67; H, 7.46; N, 12.55.

4.1.3.8. 5-Formyl-1-methyl-1H-pyrrole-2-carboxylic acid [(S)-1-((S)-1-formyl-3-methyl-butylcarbamoyl)-2-methyl-propyl]-amide (11).

Oxidation of **30** according to general procedure C gave **11** as an orange solid (150 mg, 75%). Mp 134–136 °C; HRMS (ES^+) calcd for $\text{C}_{18}\text{H}_{28}\text{N}_3\text{O}_4$ ($\text{M}+\text{H}^+$) 350.2080 found 350.2086; v_{max} (KBr) 1741 (CHO); ^1H NMR (500 MHz, CDCl_3) 0.87 (3H, d, $J = 7.0$ Hz, CH_3), 0.92 (3H, d, $J = 7.0$ Hz, CH_3), 0.96 (3H, d, $J = 7.0$ Hz, CH_3), 1.00 (3H, d, $J = 7.0$ Hz, CH_3), 1.43–1.48 (1H, m, $\text{CH}_2\text{CH}(\text{CH}_3)_2$), 1.70–1.77 (2H, m, $\text{CH}_2\text{CH}(\text{CH}_3)_2$), 2.14–2.24 (1H, m, $\text{CH}(\text{CH}_3)_2$), 4.21 (3H, s, NCH_3), 4.41–4.44 (1H, m, $\text{CHCH}_2\text{CH}(\text{CH}_3)_2$), 4.62 (1H, app t, $J = 8.0$ Hz, $\text{CHCH}(\text{CH}_3)_2$), 6.19 (1H, d, $J = 8.0$ Hz, NH), 6.61–6.66 (1H, m, CHCH), 6.88 (1H, d, $J = 4.0$ Hz, NH), 7.25–7.27 (1H, m, CHCCHO), 9.69 (1H, s, CHO), 9.70 (1H, s, CHO); ^{13}C NMR (75 MHz, CDCl_3); 18.5 (CH_3), 19.5 (CH_3), 22.1 (CH_3), 23.3 (CH_3), 25.1 ($\text{CHCH}_2\text{CH}(\text{CH}_3)_2$), 31.7 ($\text{CHCH}(\text{CH}_3)_2$), 38.1 ($\text{CHCH}_2\text{CH}(\text{CH}_3)_2$), 57.8 ($\text{CHCH}_2\text{CH}(\text{CH}_3)_2$), 58.7 ($\text{CHCH}(\text{CH}_3)_2$), 64.0 (NCH_3) 112.1 (CHCH), 122.5, (CHCCHO), 128.6 (CCONH), 130.1 (CNCH₃), 181.2 (CONH), 185.7 (CONH), 199.6 (CCHO), 199.0 (CHCHO); m/z (ES) 350 $[\text{M}+(\text{H})]^+$, 100%. Anal. Calcd for $\text{C}_{18}\text{H}_{27}\text{N}_3\text{O}_4$: C, 61.87; H, 7.79; N, 12.03. Found C, 62.11; H, 8.11; N, 11.98.

4.1.3.9. 5-Methyl-1H-pyrrole-2-carboxylic acid [(S)-1-((S)-1-formyl-3-methyl-butylcarbamoyl)-2-methyl-propyl]-amide (12).

Oxidation of **31** according to general procedure C gave **12** as a colourless solid (90 mg, 63%). Mp 159–161 °C; HRMS (ES^+) calcd for $\text{C}_{17}\text{H}_{29}\text{N}_3\text{O}_3$ ($\text{M}+\text{H}^+$) 322.2131 found 322.2141; v_{max} (KBr) 1736 (CHO); ^1H NMR (500 MHz, CDCl_3) 0.85 (3H, d, $J = 7.0$ Hz, CH_3), 0.90 (3H, d, $J = 7.0$ Hz, CH_3), 0.99 (3H, d, $J = 7.0$ Hz, CH_3), 1.01 (3H, d, $J = 7.0$ Hz, CH_3), 1.24–1.27 (1H, m, $\text{CH}_2\text{CH}(\text{CH}_3)_2$), 1.63–1.69 (2H, m, $\text{CH}_2\text{CH}(\text{CH}_3)_2$), 2.18–2.20 (1H, m, $\text{CH}(\text{CH}_3)_2$), 2.30 (3H, s, CCH_3) 3.66–3.68 (1H, m, $\text{CHCH}_2\text{CH}(\text{CH}_3)_2$), 4.57–4.62 (1H, m, $\text{CHCH}(\text{CH}_3)_2$), 5.94 (1H, br s, CHCH), 6.45 (1H, br s, NH), 7.25–7.27 (1H, m, CHCCH_3), 7.32 (1H, br s, NH), 9.59 (1H, s, CHO); ^{13}C NMR (75 MHz, CDCl_3) 16.5 (CH_3), 18.6 (CH_3), 19.0 (CH_3), 22.9 (CH_3), 23.8 ($\text{CHCH}_2\text{CH}(\text{CH}_3)_2$), 30.8 ($\text{CHCH}(\text{CH}_3)_2$), 36.3 ($\text{CHCH}_2\text{CH}(\text{CH}_3)_2$), 60.6 ($\text{CHCH}_2\text{CH}(\text{CH}_3)_2$), 66.8 ($\text{CHCH}(\text{CH}_3)_2$), 105.5 (CH_3), 126.3 (CHCH), 128.0 (CHCH), 135.0 (CCH_3), 158.0 (CONH), 169.3 (CONH); 199.6 (CHO); m/z (ES) 322 $[\text{M}+(\text{H})]^+$, 100%. Anal. Calcd for $\text{C}_{17}\text{H}_{27}\text{N}_3\text{O}_3$: C, 63.53; H, 8.47; N, 13.07. Found C, 63.90; H, 8.22; N, 12.70.

4.1.3.10. 5-[(S)-1-((S)-1-Formyl-3-methyl-butylcarbamoyl)-2-methyl-propylcarbamoyl]-1H-pyrrole-2-carboxylic acid methyl ester (13). Oxidation of **32** according to general procedure C gave

13 as a colourless solid (0.33 g, 69%). Mp 93–95 °C; HRMS (ES⁺) calcd for C₁₈H₂₈N₃O₅ (M+H⁺) 366.2029 found 366.2033; ν_{max} (KBr) 1736 (CHO); ¹H NMR (500 MHz, CDCl₃) 0.84 (3H, d, *J* = 6.1 Hz, CH₃), 0.86 (3H, d, *J* = 6.1 Hz, CH₃), 0.99 (3H, d, *J* = 6.6 Hz, CH₃), 1.02 (3H, d, *J* = 6.6 Hz, CH₃), 1.38–1.45 (1H, m, CH₂CH(CH₃)₂), 1.60–1.72 (2H, m, CH₂CH(CH₃)₂), 2.12–2.22 (1H, m, CH(CH₃)₂), 3.86 (1H, s, OCH₃), 4.48–4.55 (1H, m, CHCH₂CH(CH₃)₂), 4.64 (1H, app t, *J* = 8.5 Hz, CHCH(CH₃)₂), 6.72 (1H, s, CHCH), 6.84–6.87 (1H, m, CHCCOME), 7.15 (1H, d, *J* = 7.0 Hz, NH), 7.60 (1H, br s, NH), 9.54 (1H, br s, CHO), 10.85 (1H, br s, NH); ¹³C NMR (75 MHz, CDCl₃); 18.6 (CH₃), 19.6 (CH₃), 22.0 (CH₃), 23.4 (CH₃), 24.9 (CHCH₂CH(CH₃)₂), 31.6 (CHCH(CH₃)₂), 38.0 (CHCH₂CH(CH₃)₂), 57.7 (CHCH₂CH(CH₃)₂), 58.5 (CHCH(CH₃)₂), 63.9 (OCH₃), 111.8 (CHCH), 125.4, (CHCCHO), 129.9 (CCONH), 130.0 (CN), 161.5 (CONH), 171.7 (CONH), 199.9 (CHCHO); *m/z* (ES) 366 [M+H]⁺, 100%. Anal. Calcd for C₁₈H₂₇N₃O₅: C, 59.16; H, 7.45; N, 11.50. Found C, 59.41; H, 7.87; N, 11.82.

4.2. Sequencing of ovine calpains

RNA was isolated from ovine muscle tissue using an RNeasy[®] Mini Kit (Qiagen GmbH, Hilden, Germany) as per the manufacturer's instructions.

Calpain 1 cDNA was synthesised following the manufacturer's protocol using oligo(dt)_{12–18} primers and Superscript III Reverse Transcriptase (Invitrogen, California, USA). The calpain I coding sequence was amplified in two fragments using gene specific primers designed on the bovine sequence (GenBank Accession No. NM174259) using DNAMAN[™] (version 4.0, Lynnon Biosoft, Quebec, Canada). The 5' amplicon PCR was carried out in a total reaction volume of 20 µL consisting of 1× PCR buffer (Invitrogen, California, USA), 4 µL Q solution (Invitrogen, California, USA), 2.5 mM MgCl₂, 250 nm forward primer (5'-ACCGTGAATTAGAGATCGTC-3'), 250 nm reverse primer (5'-ACAGGGTGGTGTCCAGTTG-3'), 125 µM dNTPs, 1 U Taq DNA Polymerase (Qiagen GmbH, Germany), 1 µL gene specific cDNA and water added up to volume. The thermo-cycling profile consisted of initial denaturation at 94 °C for 10 min, followed by 35 cycles of 94 °C for 30 s, 55 °C for 30 s, and 72 °C for 1 min and one final extension step of 72 °C for 10 min.

The 3' amplicon PCR was carried out in a total reaction volume of 20 µL consisting of 1× PCR buffer (Invitrogen, California, USA), 4 µL Q solution (Invitrogen, California, USA), 2.5 mM MgCl₂, 250 nm forward primer (5'-TCCGAGACTTCATGCGTG-3'), 250 nm reverse primer (5'-AGGCACTGTCAGCTGGTG-3'), 125 µM dNTPs, 1 U Taq DNA Polymerase (Qiagen GmbH, Germany), 1 µL gene specific cDNA and water added up to volume. The thermo-cycling profile consisted of: initial denaturation at 94 °C for 10 min, followed by 35 cycles of 94 °C for 30 s, 57 °C for 30 s, and 72 °C for 1 min and one final extension step of 72 °C for 10 min.

The 5' and 3' amplicons were sequenced several times from several animals in the forward and reverse directions using the above-mentioned primers at the Allan Wilson Centre (Massey University, Palmerston North, New Zealand).

Calpain 2 cDNA was synthesised as per the manufacturer's protocol using Superscript III Reverse Transcriptase (Invitrogen, California, USA) and a calpain 2 gene specific 3' primer (5'-AAAAGTTTCTCCGTGGAGGCT-3'). Calpain 2 was then amplified by PCR using primers flanking the coding region designed from the rat sequence (GenBank Accession No. NM017116) using DNAMAN[™] (version 4.0, Lynnon Biosoft, Quebec, Canada). PCRs were carried out in a total reaction volume of 25 µL consisting of 1× PCR× Enhancer Buffer (Invitrogen, California, USA), 200 µM dNTPs, 1.5 mM MgCl₂, 200 nM forward primer (5'-GACGACCATGGCGGGCATCGCGGCC-3'), 200 nM reverse primer (5'-ATTAACAAGCTTCAAAGTACTGAAAAACAC-3'), 5 µL PCR× Enhancer Solution (Invitrogen, California, USA), 1 U Platinum[®] Taq DNA Polymerase High

Fidelity (Invitrogen, California, USA), 1 µL gene specific cDNA and water added up to volume. The samples were amplified using the following parameters: initial denaturation at 94 °C for 10 min, followed by 35 cycles of 94 °C for 30 s, 55 °C for 30 s, and 68 °C for 3 min followed by a final extension at 72 °C for 10 min.

PCR amplicons were sequenced several times in the forward and reverse directions using the previously mentioned primers (along with other internal primers designed from the developing ovine sequence) at the Waikato University DNA Sequencing Facility (University of Waikato, Waikato, New Zealand). The sequences were compiled using the GeneDoc Multiple Sequence Alignment Editor & Shading Utility (version, 2.6.002, Pittsburgh Supercomputing Centre, Pittsburgh, PA, USA).

The consensus coding sequences for ovine calpain 1 (2151 bp) and calpain 2 (2103 bp) were constructed from sequence data derived from PCRs performed on several non-related animals and the calpain 2 sequence submitted to GenBank (Accession No. EU161096).

4.3. Enzyme assays

o-CAPN1 and o-CAPN2, partially purified from sheep lung by hydrophobic and ion-exchange chromatography, were diluted in a mixture containing 20 mM MOPS, 2 mM EGTA, 2 mM EDTA and 0.5% β-mercapto-ethanol (pH 7.5) to give a linear response over the course of the assay. The substrate solution (0.0005% BODIPY-FL casein in 10 mM CaCl₂, 0.1 mM NaN₃ and 0.1% β-mercapto-ethanol) was prepared fresh each day. Calpain inhibition assays were performed in 96-well black Whatman[®] plates at 25 °C. Calpain control assays contained 50 µL of enzyme and 50 µL of sample buffer. The reaction was initiated by the addition of 100 µL of substrate solution. The progress of the reaction was followed for 10 min in a (BMG) Fluorostar with excitation at 485 nm and emission at 530 nm. For inhibitor assays the sample buffer was replaced with 50 µL of inhibitor dissolved in DMSO (2% total concentration) and diluted with water. The percentage inhibition was determined as 100 times the activity with inhibitor present divided by the activity of the control assay. The reported IC₅₀ values are the average of triplicate determinations.

4.4. Lens culture

The EMEM culture medium for normal culture (EMEM, pH 7.4) was prepared from minimum essential medium powder (or MEM, purchased from Sigma, product number M0643, 2003), 26 mM NaHCO₃, 0.02 mg/mL gentamycin (antibiotic, from Sigma) and 2.5 µg/mL amphotericin B (anti-fungal, from Sigma) in dH₂O. The culture medium was immediately sterilised by filtering with 0.2 µm pore size filters into autoclaved bottles. 2 M Ca²⁺ solution in sterilised dH₂O was added to 10 mL culture medium to give a final concentration of 5 mM Ca²⁺. Calpain inhibitors were solubilised in DMSO to give a final concentration of DMSO in EMEM of less than 0.05%. Adequate amounts of DMSO were added to the medium containing 5 mM Ca²⁺ so there was no effect attributed by DMSO. Groups of ovine eye globes from 9 to 12 month old lambs were collected from a local slaughterhouse immediately after slaughter and delivered to the laboratory for lens dissection. Pairs of lenses from the eyes of each animal were kept together. Three pairs of lenses were dissected within 2 h of death of the animal using the posterior approach. The intact lenses were immediately placed in a sterile culture dish containing 10 mL of culture medium per lens. The entire lens was submerged with its anterior epithelium facing upward in the medium, which had been pre-incubated at 37 °C with 5% CO₂ for 48 h in a sterilised chamber. One of each of the paired lenses was pre-incubated with **9** (10 µM) in EMEM for 2.5 h, whilst the other was cultured in EMEM only. Both lenses

were then exposed to a final concentration of 5 mM Ca^{2+} in EMEM, by the addition of 16 μL of 2 M Ca^{2+} stock solution in dH_2O . All lenses were incubated at 37 °C under 5% CO_2 for 44 h. All the lenses were then photographed using a digital camera (Sony Cybershot DSCF505V) fitted to a stand. A transparent flat bottom culture dish containing a lens and medium was placed on black grid lines ($1 \times 1 \text{ mm}$) with a white background light. Images of the anterior epithelium of the lens were taken with an image resolution of 1856×1392 pixels as a RGB true colour JPEG image. The lens opacity grade was scored by an image analysis system that was programmed to grade the extent of opacification captured by a digital photo image. The software used to grade the opacification captured was Image Pro-Plus v 4.1. A macro-script was created to automatically analyse the digital images of lenses (pixel size 1856×1392) placed on a $1 \text{ mm} \times 1 \text{ mm}$ black grid. The grading system was developed on the basis of selecting predefined pixel RGB values, after area defining and sharpening of the image. Lenses were graded on a scale of 1 to 100, with fully opaque lens scoring 100 and transparent lens 1.

4.5. Molecular modelling

All molecular modelling experiments were conducted with the Schrödinger suite, 2005. Conformational searches on **4–13** were carried out with MacroModel 9.1,³³ generating an ensemble of low energy conformers to establish suitable starting conformations of each compound for the docking studies. The searches were conducted with the MCMM method using a GB/SA water model and the OPLS2001 force field, with 3000 steps for the conformational search and up to 5000 iterations for the minimisation of each generated structure. The minimisation was stopped with the default gradient convergence threshold of $d = 0.05 \text{ kJ}/(\text{mol } \text{\AA})$. The default Polak-Ribiere Conjugate gradient method was used for all minimisations. The crystal structure of human mini calpain 1 (PDB code 1ZCM)²⁹ was prepared for use in the modelling studies using the protein preparation facility in GLIDE 4.0³⁴ followed by deprotonation of Cys₁₁₅ and protonation of His₂₇₂. The in silico ovine homology models were created by the virtual mutation of the appropriate residues around the active site cleft. These structures were minimised using the OPLS2005 force field with a GB/SA water model over 500 iterations. All residues within a 5 Å distance to the calcium ions, the calcium ions and the key residues Gly₂₀₈ Gly₂₇₁ and Cys₁₁₅ (o-CAPN1) or Gly₁₉₈, Gly₂₆₁ and Cys₁₀₅ (o-CAPN2) of the structures were kept frozen during this minimisation. The centre of the docking grid was defined as the centroid of the residues Cys₁₁₅, Gly₂₀₈, and Gly₂₇₁ (o-CAPN1) or Gly₁₉₈, Gly₂₆₁ and Cys₁₀₅ (o-CAPN2) and was generated with GLIDE 4.0 using default settings. The centre of the docked ligands was defined within a 12 Å box. The docking of flexible ligands to the rigid calpain model with GLIDE 4.0 was performed with the following parameters: OPLS2001 force field, extra precision mode, 90,000 poses per ligand for the initial docking, keep best 1000 poses per ligand for energy minimisation, energy minimisation with a distance dependent dielectric constant of 2 and a maximum of 5000 conjugate gradient steps.

For the docking studies of **4–13** a conformational search was conducted for each compound and X-cluster used to choose representative conformers from the ensemble within a 12 kJ/mole of the global minimum. These, usually three to five, were used as starting conformers in the docking studies. From each docking study up to ten poses as defined by the program were collected. Representative poses were chosen such that (i) the distance between the carbonyl carbon of the aldehyde group and the active site cysteine sulfur is less than 4.5 Å; (ii) *trans* Val amide bonds were preferred³⁶ to *cis* (iii) appropriate hydrogen bonds in the active site are present and (iv) poses have a low energy Glide *E*model score. The associated

parameters of the most representative poses of compounds **4–13** docked to the o-CAPN1 and o-CAPN2 homology models are shown in Table 2.

Acknowledgments

We thank Matthew Muir for the supply of calpain and Dr. Quentin MacDonald (QBit NZ) for helpful discussions. The research was supported by a University of Canterbury Fellowship (A.T.N., S.G.A.), grants from the New Zealand Public Good Science and Technology Fund LINX205 (including support for M.A.J., J.M.M.), a Tertiary Education Commission enterprise scholarship (HYYL), the Foundation for Research Science and Technology (SBM) and Douglas Pharmaceuticals Limited.

References and notes

- Goll, D.; Thompson, V. F.; Li, H.; Wei, W.; Cong, J. *J. Physiol. Rev.* **2003**, *83*, 731–801.
- Huang, Y.; Wang, K. K. W. *Trends Mol. Med.* **2001**, *7*, 355–362.
- Duncan, G.; Bushell, A. R. *Exp. Eye Res.* **1975**, *20*, 223–230.
- Sanderson, J.; Marcantonio, J. M.; Duncan, G. *Invest. Ophthalmol. Vis. Sci.* **2000**, *41*, 2255–2261.
- Robertson, L. J. G.; Morton, J. D.; Yamaguchi, M.; Bickerstaffe, R.; Shearer, T. R.; Azuma, M. *Invest. Ophthalmol. Vis. Sci.* **2005**, *46*, 4634–4640.
- Nam, D. H.; Lee, K. S.; Kim, S. H.; Kim, S. M.; Jung, S. Y.; Chung, S. H.; Kim, H. J.; Kim, N. D.; Jin, C.; Lee, Y. S. *Bioorg. Med. Chem. Lett.* **2008**, *18*, 205–209.
- Tully, D. C.; Liu, H.; Chatterjee, A. K.; Alper, P. B.; Epple, R.; Williams, J. A.; Roberts, M. J.; Woodmansee, D. H.; Masick, B. T.; Tumanut, C.; Li, J.; Spraggon, G.; Hornsby, M.; Chang, J.; Tuntland, T.; Hollenbeck, T.; Gordon, P.; Harris, J. L.; Karanewsky, D. S. *Bioorg. Med. Chem. Lett.* **2006**, *16*, 5112–5117.
- Palmer, J. T.; Bryant, C.; Wang, D.-X.; Davis, D. E.; Setti, E. L.; Rydzewski, R. M.; Venkatraman, S.; Tian, Z.-Q.; Burrill, L. C.; Mendonca, R. V.; Springman, E.; McCarter, J.; Chung, T.; Cheung, H.; Janc, J. W.; McGrath, M.; Somoza, J. R.; Enriquez, P.; Yu, Z. W.; Strickley, R. M.; Liu, L.; Venuti, M. C.; Percival, M. D.; Falgoutyret, J.-P.; Prasit, P.; Oballa, R.; Riendeau, D.; Young, R. N.; Wesolowski, G.; Rodan, S. B.; Johnson, C.; Kimmel, D. B.; Rodan, G. *J. Med. Chem.* **2005**, *48*, 7520–7534.
- Lampi, K. J.; Kadoya, K.; Azuma, M.; David, L. L.; Shearer, T. R. *Toxicol. Appl. Pharmacol.* **2005**, *117*, 53–57.
- Sanderson, J.; Marcantonio, J. M.; Duncan, G. *Biochem. Biophys. Res. Commun.* **1996**, *218*, 893–901.
- Tamada, Y.; Fukiage, C.; Mizutani, K.; Yamaguchi, M.; Nakamura, Y.; Azuma, M.; Shearer, T. R. *Curr. Eye Res.* **2001**, *22*, 280–285.
- Inomata, M.; Hayashi, M.; Shumiyu, S.; Kawashima, S.; Ito, Y. *J. Biochem.* **2000**, *128*, 771–776.
- Augusteyn, R. C.; Stevens, A. *Prog. Polym. Sci.* **1998**, *23*, 375–413.
- Kuszak, J. R.; Mazurkiewicz, M.; Jison, L.; Madurski, A.; Ngando, A.; Zoltoski, R. K. *Vet. Ophthalmol.* **2006**, *9*, 266–280.
- Robertson, L. J. G.; David, L. L.; Riviere, M. A.; Wilmarth, P. A.; Muir, M. S.; Morton, J. D. *Invest. Ophthalmol. Vis. Sci.* **2008**, *49*, 1016–1022.
- Abell, A. D.; Jones, M. A.; Neffe, A. T.; Aitken, S. G.; Cain, T. P.; Payne, R. J.; McNabb, S. B.; Coxon, J. M.; Stuart, B. G.; Pearson, D.; Lee, H. Y.-Y.; Morton, J. D. *J. Med. Chem.* **2007**, *50*, 2916–2920.
- Optimal yield of the desired dipeptide alcohols **16–20** was obtained using 1.2 equiv of **15**.
- Parikh, J. R.; Doering, W. v. E. *J. Am. Chem. Soc.* **1967**, *89*, 5505–5507.
- Sun, L.; Cui, J.; Liang, C.; Zhou, Y.; Nematala, A.; Wang, X.; Chen, H.; Tang, C.; Wei, J. *Bioorg. Med. Chem. Lett.* **2002**, *12*, 2153–2157.
- Barker, P.; Gendler, P.; Rapoport, H. J. *Org. Chem.* **1978**, *43*, 4849–4853.
- Curran, T. P.; Keaney, M. T. *J. Org. Chem.* **1996**, *61*, 9068–9069.
- Aoki, K.; Imajoh, S.; Ohno, S.; Emori, Y.; Koike, M.; Kosaki, G.; Suzuki, K. *FEBS Lett.* **1986**, *205*, 313–317.
- Imajoh, S.; Aoki, K.; Ohno, S.; Emori, Y.; Kawasaki, H.; Sugihara, H.; Suzuki, K. *Biochemistry* **1988**, *27*, 8122–8128.
- Sorimachi, H.; Amano, S.; Ishiura, S.; Suzuki, K. *Biochim. Biophys. Acta* **1996**, *1309*, 37–41.
- Deluca, C. I.; Davies, P. L.; Samis, J. A.; Elce, J. S. *Biochim. Biophys. Acta* **1993**, *1216*, 81–93.
- Thompson, V. F.; Saldana, S.; Cong, J.; Goll, D. E. *Anal. Biochem.* **2000**, *279*, 170–178.
- Inoue, J.; Nakamura, M.; Cui, Y.-S.; Sakai, Y.; Sakai, O.; Hill, J. R.; Wang, K. W. W.; Yuen, P.-W. *J. Med. Chem.* **2003**, *46*, 868–871.
- Mehdi, S.; Angelastro, M. R.; Wiseman, J. S.; Bey, P. *Biochem. Biophys. Res. Commun.* **1988**, *157*.
- Li, Qingshan, Q.; Hanzlik, R. P.; Weaver, R. F.; Schönbrunn, E. *Biochemistry* **2006**, *45*, 701–708.
- PBD file numbers: 1MDW, 1TL9, 1TLO, 1KXR, 2G8J, 2G8E, 2NQG, 2NQI, 2ARY, 1ZCM.
- Moldoveanu, T.; Hosfield, C. M.; Lim, D.; Jia, Z.; Davies, P. L. *Nat. Struct. Biol.* **2003**, *10*, 371–378.

32. Davis, T. L.; Walker, J. R.; Finerty, P. J.; Mackenzie, F.; Newman, E. M.; Dhe-Paganon, S. J. *Mol. Biol.* **2007**, 366, 216–229.
33. MacroModel, version 9.1, Schrödinger, LLC, New York, NY, 2005.
34. Glide, version 4.0, Schrödinger, LLC, New York, NY, 2005.
35. Calpain inhibitors typically adopt a β -strand conformation that spans ca. 15 Å of the active site cleft of calpain. An X-ray structure of leupeptin co-crystallised with r-CAPN1 construct (PDB code 1TL9) shows two key hydrogen bonds between the NH and carbonyl groups of Leu (P2) and Gly₂₀₈ and also an additional hydrogen bond between the NH of the P1-P2 amide bond and Gly₂₇₁. Recent X-ray crystal structures, for example, SNJ1715 co-crystallised with r-CAPN1 construct (PDB code 2G8E), confirm the importance of these hydrogen bonds. These hydrogen bonds equate to the hydrogen bonds labelled A, B and C as reported in Table 2.
36. The Leu amide in all of the docked compounds **4–13** is *trans* in all poses. We did not limit the programme to collecting only poses where the amide(s) is *trans* and for some poses the Val amine is in a *cis* configuration.
37. Of the 84 poses generated for inhibitor **8** docked in the o-CAPN1 and o-CAPN2 models, 72 gave the carbonyl carbon of the aldehyde in proximity to the active site cysteine (<4.5 Å). Of these 72 poses 42 exhibited a β -strand arrangement of the inhibitor and 20 of these had the Val amide in a *trans* configuration.
38. Of the 32 poses generated for inhibitor **9** docked in o-CAPN2 model only six gave the carbonyl carbon of the aldehyde in proximity to the active site cysteine (<4.5 Å). Of these six poses five including the lowest energy poses were in the shunted arrangement with only a single pose with the inhibitor in a more common binding mode as defined by hydrogen bonds A, B and C.
39. The 5-formyl-pyrrole **9** possesses two aldehyde groups. Only two of the 72 poses collected in the docking studies with o-CANP1 and o-CANP2 show the pyrrole aldehyde in proximity to the active site cysteine sulfur (<4.5 Å). Thirty-three poses have the Leu aldehyde in proximity to the active site cysteine sulfur. Furthermore, the Leu aldehyde is the more reactive to nucleophilic attack since the nitrogen of the pyrrole aldehyde reduces the electrophilic character of the carbonyl. The dialdehyde **9** reacts with hydroxylamine only at the Leu aldehyde. This supports the Leu aldehyde as being responsible for the potency of **9**.
40. Glide *E*model combines the energy grid score, the binding affinity predicted by the GlideScore and the internal strain energy of the ligand for the model potential used to direct the conformational-search algorithm.
41. Glide *E*internal score is the internal strain energy of the ligand.
42. Abell, A. D.; Coxon, J. M.; Miyamoto, S.; Jones, M. A.; Neffe, A. T.; Aitken, S. G.; Stuart, B. G.; Nikkel, J. M.; Morton, J. D.; Bickerstaffe, R.; Robertson, L. J.; Lee, H. Y.; Muir, M. S. N.Z. Patent. 2007, 547303; U.S. Patent Appl., 2007, 20070293560.